



Review

A Review of Terrestrial Carbon Assessment Methods Using Geo-Spatial Technologies with Emphasis on Arid Lands

Salem Issa ^{1,*}, Basam Dahy ¹, Taoufik Ksiksi ² and Nazmi Saleous ³

¹ Department of Geosciences, College of Science, UAE University, Al Ain, UAE; basam.d@uaeu.ac.ae

² Department of Biology, College of Science, UAE University, Al Ain, UAE; tksiksi@uaeu.ac.ae

³ Department of Geography, College of Science, UAE University, Al Ain, UAE; nazmi.saleous@uaeu.ac.ae

* Correspondence: salem.essa@uaeu.ac.ae

Received: 18 April 2020; Accepted: 18 June 2020; Published: 23 June 2020



Abstract: Geo-spatial technologies (i.e., remote sensing (RS) and Geographic Information Systems (GIS)) offer the means to enable a rapid assessment of terrestrial carbon stock (CS) over large areas. The utilization of an integrated RS-GIS approach for above ground biomass (AGB) estimation and precision carbon management is a timely and cost-effective solution for implementing appropriate management strategies at a localized and regional scale. The current study reviews various RS-related techniques used in the CS assessment, with emphasis on arid lands, and provides insight into the associated challenges, opportunities and future trends. The study examines the traditional methods and highlights their limitations. It explores recent and developing techniques, and identifies the most significant RS variables in depicting biophysical predictors. It further demonstrates the usefulness of geo-spatial technologies for assessing terrestrial CS, especially in arid lands. RS of vegetation in these ecosystems is constrained by unique challenges specific to their environmental conditions, leading to high inaccuracies when applying biomass estimation techniques developed for other ecosystems. This study reviews and highlights advantages and limitations of the various techniques and sensors, including optical, RADAR and LiDAR, that have been extensively used to estimate AGB and assess CS with RS data. Other new methods are introduced and discussed as well. Finally, the study highpoints the need for further work to fill the gaps and overcome limitations in using these emerging techniques for precision carbon management. Geo-spatial technologies are shown to be a valuable tool for estimating carbon sequestered especially in difficult and remote areas such as arid land.

Keywords: forest biomass; biophysical parameters; GIS; remote sensing; carbon sequestration; carbon stock

1. Introduction

Carbon sequestration is the process of capturing CO₂ gas in the atmosphere and storing it in liquid or solid state. This process occurs naturally through trees, oceans, soil, and live organic matter [1]. Any reservoirs or stores of carbon are called carbon pools. Storing of CO₂ occurs at three levels: in plants and soil (Terrestrial Sequestration), underground (Geological Sequestration) and deep in Oceans (Ocean Sequestration) (Figure 1). The bulk of carbon sequestered terrestrially is stored in forest biomass. A practical definition of forest biomass is the total amount of aboveground living organic matter in trees expressed as oven-dry tons per unit area [2]. The estimation of biomass is a challenging task, especially in the areas with both complex stands and varying environmental conditions as well as in low vegetation cover density areas, such as arid lands. Both types of ecosystems require the use of accurate and consistent measurement methods.

Arid lands in particular, have received less attention in recent decades despite their importance to society and their exceptional vulnerability to climate change. They provide ecosystem services to more than two billion people, including significant crop production and forage for wildlife and domestic livestock [3]. While arid lands are sparsely vegetated with low annual productivity, they have been identified as an important player in the global trends and variability in atmospheric CO₂ concentrations [4–7]. Monitoring the spatiotemporal dynamics of arid lands ecosystem structure and function is, therefore, a high research priority. Satellite RS particularly, has been instrumental in exposing the role of arid lands within the context of global carbon cycling and the broader Earth system [6,7].

Estimation of terrestrial carbon stock through remote sensing techniques is based on the estimation of terrestrial biomass. Terrestrial or biologic sequestration is the process of storing atmospheric CO₂ as carbon in the stems, roots of plants and soil. Forests' biotic components and soil act as large carbon pools where CO₂ in the atmosphere is converted into plant biomass through photosynthesis. Carbon sequestration through forests is estimated at 2–4 gigatons annually [8]. However, around 60% of carbon sequestered by forests is returned to the atmosphere as a result of deforestation [9]. Precise carbon stock estimation is necessary for planning carbon emission mitigation strategies and programs at the local and regional levels [10]. Studies based on such estimation are important for a better understanding of long-term behavior and drivers of carbon sequestration under the global change and land-use and land-cover change scenarios [11].

The importance of monitoring carbon and vegetation biomass has been recognized by the Paris Agreement which was signed by 197 countries, and ratified by 189 nations who have all committed to report their carbon footprint [12]. Forests, as both carbon sources and sinks, can play a major role in combating global climate change [13,14]. Afforestation projects and land use conversion to forests can be used to earn carbon credits and reduce the carbon footprint, resulting in a long-term reduction in greenhouse gas (GHGs) levels through carbon sequestration [15]. This approach has attracted a growing interest among policymakers and governments. Similarly, plantation cropping projects, as a land use system, have the potential to contribute to carbon stocks, maintain soil biodiversity and improve soil fertility [16]. These projects can add economic value as well, by providing more job opportunities, better income and food security, especially in the smallholder systems in developing countries [15,17]. Such countries can also take part in the UN program on reduction in emissions from deforestation and forest degradation (REDD+) which allows for earning financial incentives by implementing climate policies and demonstrating emission reductions through carbon sequestration [18].

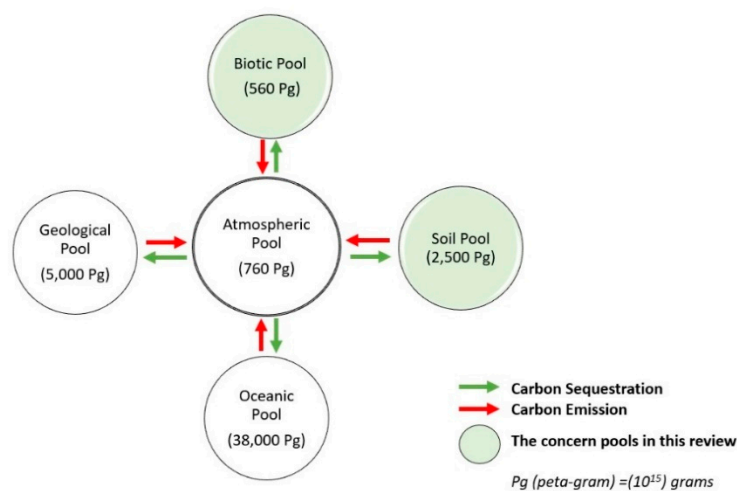


Figure 1. Carbon pools including: (1) Terrestrial Sequestration pool (sequestering and storing of CO₂ in plants and soil); (2) Geological Sequestration (underground) pool; (3) Ocean Sequestration (deep in oceans) pool; and (4) Atmospheric pool. Modified after [19].

Measuring and mapping biomass accurately are serious challenges, particularly in arid lands, that must be addressed when quantifying carbon stocks. The total carbon stock in any terrestrial ecosystem is the sum of carbon in living, dead, and soil biomass [20]. Eggleston et al. [21] have listed five terrestrial ecosystem carbon pools involving biomass: above-ground biomass (AGB), below-ground biomass (BGB), litter, woody debris and soil organic matter (SOM). Of these, AGB is the most visible, dominant, dynamic and important pool of the terrestrial ecosystem, constituting around 30% of the total terrestrial ecosystem carbon pool [22]. AGB and, especially, forest biomass estimation has received considerable attention over the last few decades because of the increased awareness of global warming and the role of forests in carbon sequestration. Furthermore, the acceleration of the release of GHGs into the atmosphere specifically from deforestation has led to numerous studies investigating the methods for the estimation and quantification of carbon stored in forests [22,23].

AGB accounts for more than 70% of total forest biomass [24]. Additionally, AGB contributes to atmospheric carbon fluxes to a much greater extent due to disturbances such as forest fires, logging and land use change, and hence has a much higher importance than the other types of biomass [25]. This implies the necessity of the continuous monitoring of AGB rather than a single date mapping. However, the estimation of AGB involves scientific challenges to identify feasible approaches to assess carbon at a national level [18]. Effective management of carbon stocks requires constant monitoring and accurate measuring of biomass [26]. The most accurate methods are the traditional biomass assessment methods based on field measurements; however, they are difficult to conduct over large areas and are not practical for broad-scale assessments [25]. They also make monitoring activities costlier, time consuming, and labor intensive. Furthermore, field-based resource inventories are usually carried out for economic, not environmental, considerations; they provide good historical data on patterns and trends, but are not accurate enough to estimate fluxes for the entire landscape and all carbon pools therein [27].

Recently, geo-spatial technologies procedures have been applied to natural resources management and biomass assessment [28,29]. RS can obtain biomass information over large areas with repetitive coverages, at a reasonable cost and with acceptable accuracy [30]. Various techniques and sensors have been used and tested in numerous studies. RS, both active and passive, provide some of the most time-efficient and cost-effective approaches to derive AGB estimation at the regional and national scale. Optical, RADAR and LiDAR data have been extensively used to estimate the same with a variety of methods. Moreover, the integration of RS data into GIS models provides advantages of both technologies, allowing for adding ancillary and field data to the analysis, besides increasing reliability in estimating AGB. However, mapping vegetation for accurate measuring of biomass and assessing carbon stock (CS) is a significant challenge which needs to be addressed when quantifying carbon stock. This is most specifically for arid lands, where RS has unique challenges that are not typically encountered in other sub-humid or humid regions. Major challenges include low vegetation signal-to-noise ratios, high soil background reflectance, presence of biological soil crusts, high spatial heterogeneity from plot to regional scales, and irregular growing seasons due to unpredictable seasonal rainfall and frequent periods of drought [3,31–33]. Additionally, there is a relative discontinuity in the long-term measurements in arid lands, which hampers reliable calibration and evaluation of remotely sensed data products. Consequently, RS techniques developed in other ecosystems often result in inaccurate estimates of arid lands ecosystem carbon stocks. To address these challenges, other innovative approaches and techniques are proposed (Section 8).

The overall objective of this review is to evaluate all spectra of methods and approaches that use geo-spatial technologies, as innovative techniques applied to biomass studies and carbon stock (CS) assessment worldwide, in particular in arid land ecosystems. The study reviews briefly traditional biomass assessment methods including destructive and allometric equations-based approaches, and summarizes their benefits and limitations. Specific objectives of the review include:

- i. To summarize traditional methods used for biomass and carbon assessment in terrestrial ecosystems;

- ii. To highlight the growing developments in biomass and terrestrial carbon stock assessment through the use of geo-spatial technologies with emphasis on arid lands;
- iii. To identify significant RS variables sensitive to measurable biophysical predictors;
- iv. To identify the gaps and limitations of RS-GIS based methods as well as to address the need for further work to overcome them.

To achieve these objectives, we start by overviewing the traditional methods used to estimate the stored carbon components in terrestrial ecosystems, including the destructive and nondestructive (allometry) methods, and their limitations. Next, we review extensively the geo-spatial technologies approach for estimating terrestrial biomass and carbon stock—which is the main focus of the current review—and assess their long-term potential. The study is organized as follows:

Section 1: provides an introduction and background information;

Section 2: gives an overview of the traditional methods used in biomass estimation;

Sections 3 and 4: give an overview of the geo-spatial methods used to attain a certain level of accuracy at the species/plant communities (multispecies) level;

Section 5: surveys all biophysical predictors used in RS technology;

Section 6: identifies significant RS variables;

Section 7: highlights RS-GIS integrated models;

Section 8: presents arid lands case studies with challenges and opportunities;

Section 9: identifies gaps and limitations of the geo-spatial approaches for biomass estimation and;

Section 10: presents conclusions, recommendations and the need for future work.

The review concludes by highlighting the best practices within the geo-spatial methods, presenting conclusions and providing recommendations. Figure 2 demonstrates the work methodology of the review.

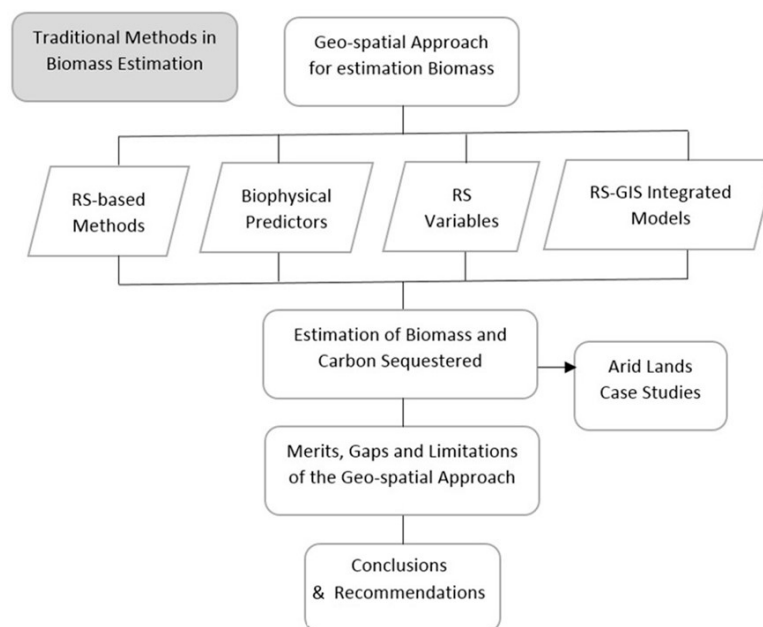


Figure 2. Workflow of the review process.

The study starts by performing a quick textual search on Google Scholar, in order to identify statistically relevant temporal patterns of the use of terms such as ‘Carbon Sequestration’, ‘Carbon Sequestration + Remote Sensing’ and ‘Carbon Sequestration + GIS’ in the literature. Statistical analysis of the data revealed an exponential increase with time in the number of scientific studies on carbon sequestration considering both RS and GIS in their methodology. This can be attributed to the

increase in volume of available satellite imagery and the ease of access to their archives witnessed over the last two decades. Furthermore, the introduction of GIS in the late eighties contributed to this trend as well. A large number of articles (387,312) were retrieved when using the term: 'Carbon Sequestration' alone. Next, this number was reduced to only 811 articles after using search keywords such as: "allometric equations", "remote sensing variables", "biophysical predictors", "GIS", "Biomass", "AGB", "vegetation indices", and "mapping". These searches were then pared down by initial reviewing of their abstract. The resulting final number was 156 articles, which were used for the preparation of this comprehensive review, considering that all reviewed articles were published in peer-reviewed journals.

2. Traditional Methods in Biomass Estimation

Plant biomass can be measured or estimated by both direct (destructive) and indirect (nondestructive) methods. Direct methods are the most accurate for determining biomass and assessing CS. This is done through destructively harvesting all plants, separating each into various constituent components (e.g., stem, branches, leaves, flowers, fruits, roots) and, subsequently, either determining the carbon content of the various components analytically or calculating this as a fraction of measured biomass (indirect) [34]. However, the destructive methods of biomass estimation are limited to a small area due to their destructive nature as well as the time, expense and labor involved. Besides, the direct methods ultimately rely on ground measurements and can result in damage to the forests, with associated environmental consequences [17,35]. The indirect methods include estimation based on allometric equations (Section 2.1) or methods that use RS/GIS-based integrated models (Sections: 4 onward).

As mentioned in Section 1 above, terrestrial carbon is calculated considering the following five components: (1) AGB; (2) BGB; (3) Litter; (4) Debris; and (5) Soil Organic Carbon (SOC) [18,21]. It is estimated as the sum of two quantities representing the amounts of carbon in biomass and in soil respectively. The first involves estimating vegetation biomass by calculating the AGB and using it to derive the remaining components, i.e., BGB, Litter and Debris, as shown in Table 1. The second involves estimating SOC, which is part of the SOM. As mentioned above, AGB accounts for 30% of the total terrestrial ecosystems carbon pool which, in turn, represents 70–90% of the total forest biomass [24]. Moreover, estimates of AGB can also be used to predict root biomass (BGB), which is generally estimated at 20% of the AGB based on the predictive relationship applied by many studies (Table 1) [24,36,37]. In addition, carbon stocks of dead wood or litter (e.g., felled or dead trees, dead or broken branches, leaves, etc.) in mature forests are generally assumed to be equivalent to 10 to 20% of the calculated AGB [18,38]. As for SOM, it is most commonly estimated through soil sampling at various layers; SOC is then estimated using the total combustion method, as explained in Walkley and Black [39]. The content of SOC included in SOM may change depending on many factors such as ecosystem, type of organic residues and land management. Many studies estimate SOC from SOM using the common factor of 1.724 (~58% of SOM). While this figure has been widely used in the last century, Brady and Weil [40] concluded that it probably applied only to highly stabilized humus. After conducting a statistical analysis of 481 studies, Pribyl [41] found that common conversion factor varied from 1.35 to 7.50, with a mean of 2.20. They concluded that applying a single conversion factor universally, had the potential for a serious error when used to estimate the carbon content of soils. However, recent studies have accepted a generic, quick, simple and inexpensive coefficient of 57% to estimate SOC from SOM [42].

Table 1. Calculation methods of stored carbon components in terrestrial ecosystems.

No	Component	Calculation Method	Source
1	AGB	Destructive OR Nondestructive Methods	[18]
2	BGB	20% of Above-ground biomass	[24]
3	Litters	10–20% of Above-ground biomass each	[38]
4	Debris		
5	SOC	Total combustion method	[39]

2.1. Allometric Equations

Allometric equations were developed to avoid destructing forests when estimating their biomass (Table 2). In general, an allometric equation is a statistical model to estimate the biomass of the trees using their biometrical characteristics (e.g., height, diameter at breast height (DBH) or crown size), which are easy and simple to measure [43]. The proportions between the tree height and diameter, between crown height and diameter, and between biomass and diameter, follow rules that are common to all trees grown under the same conditions; these become more useful in uniform forests or plantations with similarly aged stands [25]. The selection of appropriate and robust models, therefore, has considerable influence on the accuracy of the obtained estimates [44]. As mentioned above the aim of using allometric equations is to estimate biomass without the need to cut trees. However, these equations are based on the destructive sampling of vegetation in a given location, before they can be applied generally. In order for those equations to be validated, cutting and weighting tree components is necessary [45]. The number of trees destructively sampled to build allometric equations differs from one study to another. Currently, there is no consensus on that number, as this is often dependent on resource availability and permission to harvest trees [34]. For example, Russell [46] and Deans et al. [47] used 15 and 14 trees, while Brown et al. [48] and Khalid et al. [49] used only 8 and 10 trees, respectively to build their allometric equations. However, a recent study showed that small sample size (≤ 10) results in biased allometric equations [50].

Many allometric equations have been developed for various plant species. For example, the GlobeAllomeTree database contains over 706 equations from Europe, 2843 from North America and 1058 from Africa [51]. Some of these are volume equations, and the others are biomass equations. One of the limitations of volume equations is that they can only be applied to stems, while biomass equations cover a wide range of vegetation components [52]. Allometric models can be developed for either individual or multiple species (a mixture of species) to represent a community or bioregion. They also can be developed to cover specific sites, regional or pan-tropical scales [34,44]. Only a few biomass assessment equations are available for plant species in desert or arid land ecosystems. The multispecies equations are developed due to the challenges involved in developing allometric equations for all species present in the ecosystem [13]. Chave et al. [53] have shown that one hectare of a tropical forest may shelter as many as 300 different tree species. Hence, the multispecies allometric models are more methodologically efficient for biomass estimation compared to those developed for individual species at specific locations. However, these models carry the potentiality to misrepresent local, species- or community-specific variations and anomalies. Therefore, they may fail to capture variations in both forest type and the full diversity of the natural vegetation communities hence leading to an increased level of uncertainty [44]. Hence, a tailored equation for each specific species is needed for a better accuracy in estimating the biomass. Nevertheless, such an equation will still be conditioned by the ecological zone based on which it had been built. In their review of allometric equations in Asia, Yuen et al. [34] concluded that applying the existing allometric equations for the sake of convenience can potentially be a key source of uncertainty in above- and below-ground carbon stock estimates in many Asian landscapes. Site and species-specific allometric models could provide a higher level of accuracy at a given location to assist with the assessment of biomass carbon sequestration. This will make the locally developed equation a better option allowing to produce a more accurate and

site-specific biomass estimation [35]. Since the choice of the equation is the first critical step in this process, there has been a rapid increase in efforts to develop locally appropriate equations [51].

Most equations for AGB or biomass of any component (stem, branch, leaves, other) consider the diameter and/or height as the independent variables. In their study to investigate the allometric equations in China, Cheng et al. [52] found that the most frequently used predictive variable in single-variable models was the DBH, and those in two-variable models were DBH and tree height while wood density and CD were used in more complex models. They found that diameter variables had a dominant proportion of 87.4% of the surveyed equations. However, DBH showed a weak correlation with biomass quantity in certain species, such as palm trees [54,55]. Age can be used as a predictor for biomass estimation in many studies since there is a linear correlation between biomass accumulation and age [15,56]. Many studies have highlighted the importance of tree height as a predictor variable in the AGB equation [16,17,23,43]. The use of crown variables as indicators for biomass estimation became of more interest lately due to the developments in RS technologies. A single plant species can have more than one allometric equation, e.g., palm species (Table 2). More recently, allometric equations have been coupled with RS and field-based structural variables measurements [23,57–59]. Furthermore, Cheng et al. [52] recommended developing more equations with different field structural variables that can be linked to RS predictors. Likewise, Jucker et al. [60] suggested developing a new generation of allometric equations that could estimate biomass based on attributes which can be remotely sensed.

Table 2. Examples of several allometric equations developed for a single plant species.

Output Variable	Allometric Equations	Input Variable	Location	Source
AGB of palms (general)	$=1.697 \times 10^{-3} \times \text{DBH}^{1.754} \times \text{H}^{2.151}$	DBH and H	Colombia and Venezuela	[61]
Biomass of palms (general)	$=10.0 + 6.4 \times \text{H}$ $=4.5 + 7.7 \times \text{Ht}$	H and Ht	Tropical forests	[2]
AGB of <i>Elaeis guineensis</i>	$=725 + 197 \times \text{H}$	H	Malaysia	[49]
AGB of <i>A. inexcansum</i>	$=0.3060 \times \text{DBH}^{1.837} \times 1.035$	DBH	Mexico	[62]
Biomass of <i>Elaeis guineensis</i>	$= -0.00020823\text{Age}^4$ $+ 0.000153744\text{Age}^3 - 0.011636\text{Age}^2$ $+ 7.3219\text{Age} - 6.3934$	Age	Malaysia	[56]
AGB _{fresh} of <i>Elaeis guineensis</i>	$=1.5729 \times \text{Ht} - 8.2835$	Ht	West Africa	[63]
AGB _{dry} of <i>Elaeis guineensis</i>	$=0.3747 \times \text{Ht} + 3.6334$			
Trunk biomass of <i>E.guineensis</i>	$=0.1 \pi \times \text{TD} \times \text{H} \times (\text{DBH}/2)^2$	H, TD, DBH, W, D, and Age	Tropical region	[64]
Fronde biomass of <i>E.guineensis</i>	$=0.02 \times \text{W} \times \text{D} + 0.21$			
AGB of <i>Elaeis guineensis</i>	$=0.976 \times \text{H} + 0.0706$	H	Indonesia	[65]
AGB of <i>Euterpe precatoria</i>	$=13.59 \times \text{H} - 108.8$	H	Amazonia	[66]
AGB of palm (general)	$=0.0950 \times (\text{DF} \times \text{DBH}^2 \times \text{H})$	DF, DBH, and H	Amazonia	[66]
AGB of <i>Euterpe precatoria</i>	$=0.167 \times (\text{DBH}^2 \times \text{H} \times \text{TD})^{0.883}$	DBH, H, and TD	Amazonia	[67]
AGB of <i>Areca catechu</i>	$=0.03883 \times \text{H} \times \text{DBH}^{1.2}$	DBH and H	Malaysia	[16]
AGB of <i>Cocos nucifera</i>	$=3.7964 \times \text{H}^{1.8130}$	H	Tanzania	[68]
Crown biomass of <i>P. dactylifera</i>	$=14.034e^{0.0554 \times \text{CA}}$	Crown area	Abu Dhabi, UAE	[58]
Trunk biomass of <i>P. dactylifera</i>	$=40.725 \times \text{Ht}^{0.9719}$	Ht	Abu Dhabi, UAE	[58]

DBH is diameter at breast height, H is palm height, Ht is trunk height, TD is trunk density, W is frond width, D is frond depth, and DF is the dry to fresh weight ratio.

3. Geo-Spatial Approach for Estimating AGB

Ground-based methods for forest AGB estimation and carbon stock are generally based on plots, forest inventory, and monitoring methods that use allometric equations developed from destructive methods and in situ measurements [10,69]. As shown above, the biomass estimates derived from field data measurements were found to be the most accurate; however, it is not a practical approach for broad-scale assessments and not adequate enough to be used for mapping biomass estimation distribution at a regional scale. On the other hand, RS and related technologies have shown to be practical and cost/time-effective. RS can provide data over large areas at a fraction of the cost associated with extensive field works and enables assessment of inaccessible places. Data from RS satellites are available at various scales, from local to global, and from several different platforms. There are also different types of sensors both passive, such as optical and thermal RS sensors, and active, such as Radar and Light Detection and Ranging (LiDAR) sensors, with each having its advantages and disadvantages [22]. Likewise, GIS is a platform hosting spatial databases capable of assembling and integrating geographically referenced data, running spatial analysis, integrating various types and formats of spatial data, building spatial models enabling the prediction of future scenarios, and allowing for proper management of forests [70–72].

Our findings confirm the increase in scientific studies incorporating RS in their methodologies for carbon sequestration estimation during the study period. Remote sensing was widely used to collect information regarding forest AGB and vegetation structure, as well as to monitor and map vegetation biomass and productivity at a large scale [73–76]. As explained in the introduction section, the final number of articles used in the preparation of this comprehensive review was reduced to only 156 peer-reviewed articles (Figure 3).

Statistical analysis of the data retrieved reveals that three quarters of the studies used optical sensors (with different spatial resolutions) in their experimental sections while, the remaining used active sensors (almost equally divided between Radar and LiDAR sensors) (Figure 4). For optical sensors, half of the studies used coarse spatial resolution (>100 m) such as MODIS and SPOT VEG sensors. Around one third of the studies that used optical sensors estimated the biomass using moderate spatial resolution (~10–100 m) sensors such as: Landsat, Sentinel, IRS, and SPOT sensors, while around 20% of the studies used fine spatial resolution data (sub-meter to 5 m) such as IKONOS, Quickbird and World View sensors (Table 3).

Statistical results further showed that the number of studies that estimate AGB at plant species levels, instead of forests in general or mixed species, was increasing. Many plant species are not separable targets using RS because they are indistinguishable from other plants due to their spectral similarities. Hence, resolution concerns such as high spatial resolution (e.g., IKONOS) and high spectral resolution (e.g., hyperspectral) should be taken into account as they help resolve such ambiguities and play essential roles in the quality of the resulting maps [63]. Hyperspectral sensors showed plausible classification accuracies in mapping major forest species and predicting the susceptible areas of fruit malformation. Hebbbar et al. [77] used LISS-IV data to classify fruit trees and found that old and mature plantations were classified more accurately while young and recently planted ones (3 years or less) showed poor classification accuracy due to the mixed spectral signature, wider spacing and poor stands of plantations.

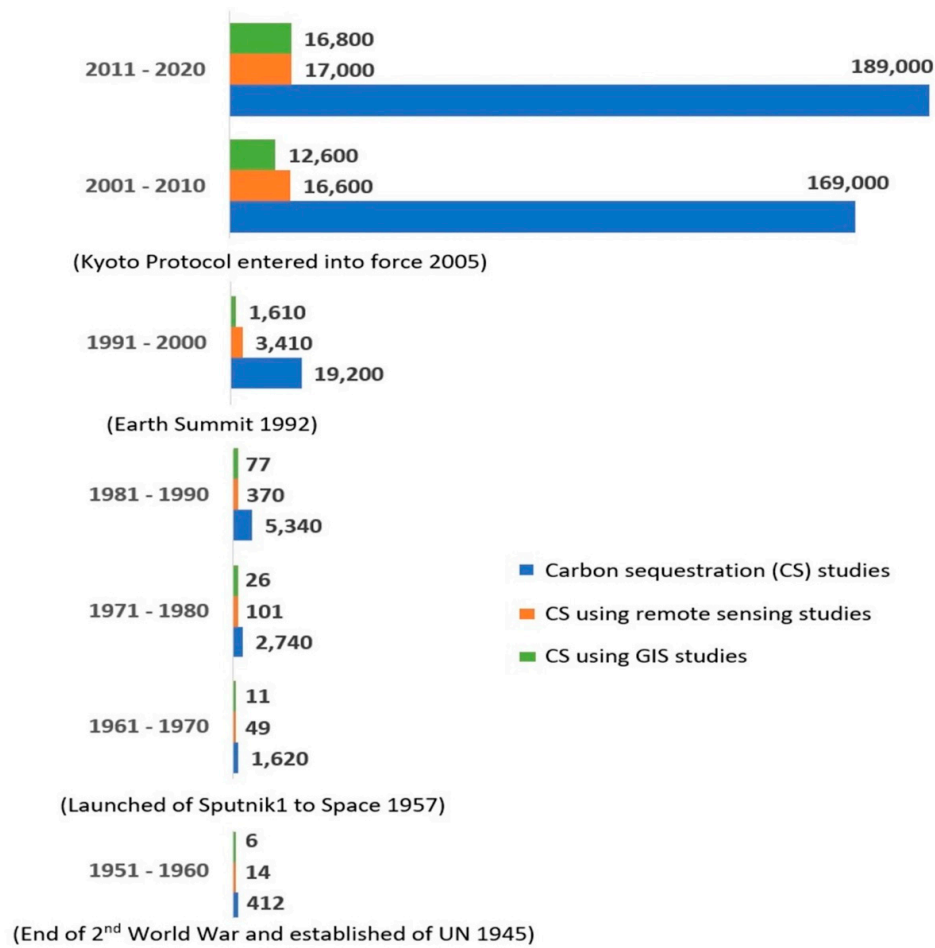


Figure 3. Textual analysis of the articles (numbers) retrieved using the terms: “carbon sequestration”, “remote sensing”, and “GIS” (Google scholar accessed on 28 h March 2020 at 08:45 AM Abu Dhabi).

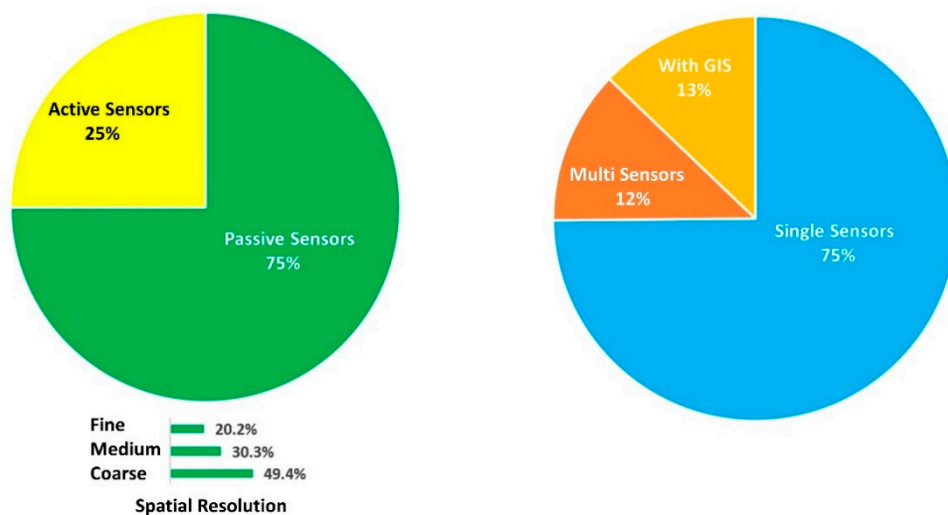


Figure 4. Sensor types, resolutions and GIS integrated methods used for the estimation of biomass and carbon sequestered, based on the 156 papers reviewed for the current study.

Table 3. Specifications of the remote sensing (RS) optical sensors most commonly used for above-ground biomass (AGB) estimation.

Sensor	Type	Bands	Spatial Resolution (m)	Temporal Resolution	Swath (km)	Cost
AVHRR	Multispectral	5 bands (Red, IR, and 3 Thermal IR)	1100	12 h	2500	Free
MODIS	Multispectral	36 bands (from Blue to Thermal IR)	250, 500 and 1000	1–2 days	2330	Free
SPOT VEG	Multispectral	4 bands (Blue, red, NIR, and SWIR)	1000	1 day	2250	Free
TM	Multispectral	7 bands (3 VIS, 3 IR and Thermal IR)	30 and 120	16 days	185	Free
ETM+	Multispectral	9 bands (3 VIS, 3 IR and 2 Thermal IR and 1 PAN)	15, 30 and 60	16 days	185	Free
SPOT	Multispectral	4 bands (2 VIS, 1 NIR, and 1 PAN)	5, 10 and 20	26 days	60	Commercial
Landsat 8 OLI	Multispectral	11 bands (1 Ultra, 3 VIS, 3 IR, 1 Cirrus, 2 Thermal IR, and 1 PAN)	15, 30 and 100	16 days	185	Free
LISS-III (IRS)	Multispectral	5 bands (2 VIS, 2 IR, and 1 PAN)	5.3, 23 and 50	5–24 days	142	Commercial
Sentinel-2	Multispectral	13 bands (4 VIS, 6 NIR and 3 SWIR)	10, 20, and 60	5–10 days	290	Free
IKONOS	Multispectral	5 bands (3 VIS, 1 IR, and 1 PAN)	1 and 4	3 days	11	Commercial
World View2	Multispectral	9 bands (6 VIS, 2 IR, 1 PAN)	1.84 and 0.46	1.1 days	16	Commercial
Quickbird	Multispectral	5 bands (4 bands and 1 PAN)	0.61 and 2.44	3 days	16	Commercial
HyMap	Hyperspectral	126 bands	2–10	Airborne	2.3 and 4.6	Commercial
AVIRIS	Hyperspectral	224 bands (from VIS to MIR)	2.5 to 20	Airborne	1.9 and 11	Commercial

Accurate image classification relies on the successful extraction of pure spectral signature for each species, which is often dictated by the spatial resolution of the observing sensor and the timing of observation [78]. Bryceson [79] used the habitat type, condition and soil type as the delineating parameters to locate *Chortoicetes terminifera* (Australian plague locust) by using Landsat-5 multispectral scanner data. Anderson et al. [80] mapped *Ericameria austrotexana* infestation in a large homogenous area using Landsat TM imagery. The spectral radiances in the red and near-infrared regions, in addition to others, were used for vegetation mapping by RS technology. The spectral signatures of photosynthetically and nonphotosynthetically active vegetation showed noticeable differences and could be utilized to estimate forage quantity and quality of grass prairies [78]. Moreover, discrimination of vegetation species from single imagery is only achievable where a combination of leaf chemistry, structure and moisture content culminates to form a unique spectral signature. As the detection and estimation of biomass are sensed from space, the crown biomass component has gained prominence in the majority of the relevant studies [52,60,81–85]. The unique pattern of crown palm plantations makes them easily distinguishable from other trees on satellite imagery [86]. Figure 5 shows the proportion of utilizing different sensors with different number of bands and costs for the estimation of the biomass and carbon sequestered. It is worth mentioning that most of these studies were conducted on boreal and tropical forests with a small portion conducted on arid regions (around 10%). This could be due to the early availability of geo-spatial technologies in the developed northern countries (boreal forests) and the relative importance of the tropical rainforests to

the global carbon cycle (Figure 5). Nowadays, RS data are widely available for a fraction of their cost only a decade ago. For example, archived and recent Landsat imageries are available and are freely downloadable from the USGS website, providing a globally consistent record of archived imageries since 1972; other resources are being continuously published and added to the internet.

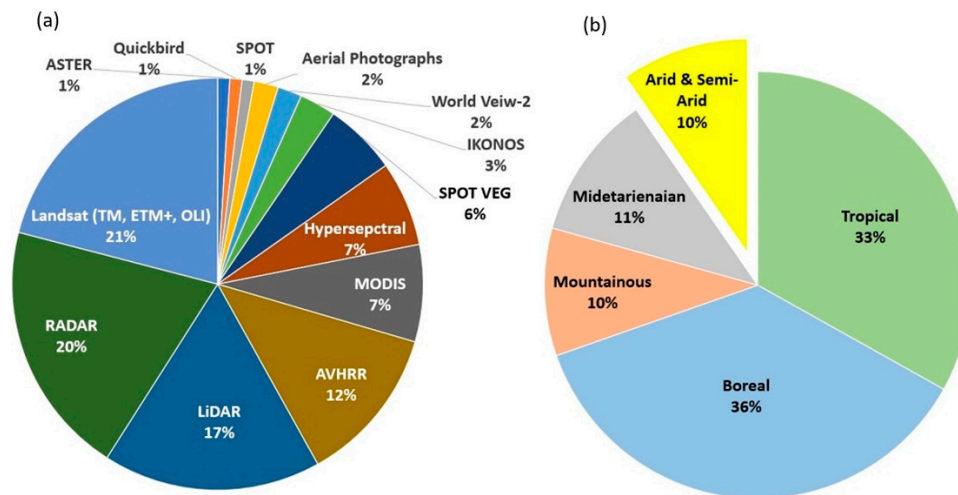


Figure 5. (a) Proportions of RS-based studies for biomass estimation and carbon sequestered in different ecoregions/forests; and (b) Sensors utilization percentages (based on the 156 studies reviewed for this paper).

4. RS-Based Methods

To explore the potential of RS-based methods to provide biomass information in different environments, various techniques and sensors have been used and tested in numerous studies. Optical, RADAR and LiDAR data have been extensively used to estimate AGB with a variety of methods [10]. AGB studies using geo-spatial technologies can be aggregated according to the level of the methodological complexity to several tiers including different levels of detail and accuracy. The Intergovernmental Panel on Climate Change (IPCC) proposed three tiers: Tier-1, Tier-2, and Tier-3 [18,87,88]. Tier-1 is the basic method based on the generalized equation or the ‘biome average’ approach. It is the simplest level using the globally available data and provides a rough approximation of biomass, and hence carbon stock, and could be used as a starting point for decision-makers; however, it can provide inaccurate results with a high level of uncertainty [18]. Tier-1 is considered as a generalized equation for the ecological zones, and is typically used when no species-specific equations exist [87]. Tier-2 is an intermediate level that is based on the volume equation and wood density. It is used when species-specific volume equations exist, and woody density for the specific plant species is available. The volume is then converted to biomass using wood density and a default biomass expansion factor (BEF) (see Section 3) [21,87]. Finally, Tier-3, the most demanding in terms of complexity and data requirements, is based on using a species-specific biomass equation to calculate either total or partial biomass. Partial biomass is obtained by adding up the biomass estimates obtained from the species-specific equations for the different compartments. Tier-2 and Tier-3 levels are more dependent on ground-based measurements of the tree (i.e., DBH and height) and building the predictive relationships (allometric equations) [18]. This makes these two levels more expensive to implement than Tier-1. It is worth noting here that the precision for a given species generally increases with the increase in the Tier number [87].

A geo-spatial approach is widely used to collect information regarding forest AGB and vegetation structure as well as to monitor and map vegetation biomass and productivity at large scales [73–76]. For mapping vegetation using RS data, a multistep process is usually applied. The first step involves image preprocessing and aims at enhancing the quality of original images. For example, satellite

data with moderate spatial resolution (such as Landsat) offers plausible results after using specific techniques such as pan-sharpening or fusion techniques, and integration with other RS sources (fine spatial resolution data or active sensors). A panchromatic band with 15 m spatial resolution that can be used to pan-sharpen other bands and hence increase their interpretability, has been added to Landsat's multispectral sensors [89,90]. Previous studies showed that such use of the panchromatic band helped achieve dramatic improvements (15%) in classification accuracies [91]. The second step involves determining the level of vegetation classification (at community or species level). The third step determines the correlation between the vegetation types and spectral characteristics of remotely sensed imagery. Vegetation data is identified by interpreting satellite images based on the elements such as image color, texture, tone, pattern and association information. Lastly, the final step includes translating the spectral classes into vegetation types by assigning each pixel of the scene to one of the vegetation groups defined in the vegetation classification system selected in the second step.

Classification methods are broadly based on the pixel-based classification (PBC) approach or the object-oriented based classification (OOC) approach. Both methods have their advantages and disadvantages depending on their areas of applications, and most importantly, the RS datasets that are used for information extraction [92]. OOC methods group several pixels with homogeneous properties into an object/objects instead of pixels, which are considered as the basic unit for analysis, while PBC approaches are based on combining reflectance pixel values into separated spectral clusters [93,94].

AGB and hence CS can be estimated from different RS data types using various approaches (Figure 6). Landsat series (i.e., TM, ETM+, OLI) have been historically used to map biomass and carbon in a variety of ecosystems, due to the relevance of their spectral bands, the continuity of the program, and the suitability of the 30 m spatial resolution for regional mapping [10]. Although biomass cannot be directly measured from space, the use of spectrally-derived parameters from sensor reflectance (bands), including vegetation indices (VIs) that were created to improve prediction accuracy, enables increased biomass prediction accuracy when combined with field-based measurements [95].

RS data have been correlated with plot-based field measurements to estimate carbon stocks. In general, RS data are empirically linked to AGB measurements of field plots using different regression analyses and algorithms [96]. There are many methods of image analysis that can be integrated to achieve a better accuracy. Algorithm development and implementation is an important subject in studies estimating biomass [25]. The advanced machine learning algorithms methods and/or other state-of-the-art processing techniques can reveal important information about the spatial and temporal biomass patterns by determining relationships between field measurements and RS data, especially over large areas [25]. To determine the relationship between above-ground field biomass and RS data, researchers have used linear regression models with or without log transformations of field biomass data, and multiple regressions with or without stepwise selection [97,98]. Artificial neural networks [99], semi-empirical models [99], nonlinear regression [100], and nonparametric estimation techniques (e.g., k-nearest neighbor and k-means clustering) have also been used [30]. However, few studies have investigated approaches other than the empirical relationship with spectral bands or VIs [101]. One of these approaches is Monteith's efficiency model for obtaining indirect estimates of absorbed photosynthetically active radiation (APAR) from the red and IR reflectance characteristics of the vegetation where APAR is used as an indication of how efficiently absorbed energy is converted to dry biomass [102]. Rosema et al. [103] used a simulation of vegetation development from daily total evapotranspiration with the in/out radiation of METESTAT in order to estimate the herbaceous biomass in savannah grassland in Sahel countries. Other studies used canopy functioning process-based models coupled with physical radiative transfer models to estimate biomass production from RS data [104]. Fourier transform textural ordination (FOTO) was used by Morel et al. [105] with SPOT5 data for estimation AGB in Thailand with the R-value equal to 0.83.

Regression, ordinary kriging, co-kriging, and stepwise linear regression have been used in various studies and it was found that the combination of RS and geo-statistics can improve the accuracy of biomass estimates more than the use stepwise linear regression only [106]. Extensive field knowledge

and expert knowledge may help improve classification accuracy. Studies have shown that classification accuracy can be greatly improved after applying expert knowledge (empirical rules) and ancillary data to extract thematic features (e.g., vegetation groups) [78]. Fieldwork is the foundation for RS technology allowing to extend limited vegetation information to large scale predictions [107]. This direct mapping approach is more accurate at depicting variations in biomass across the landscape, making it easier to update the maps as needed [108].

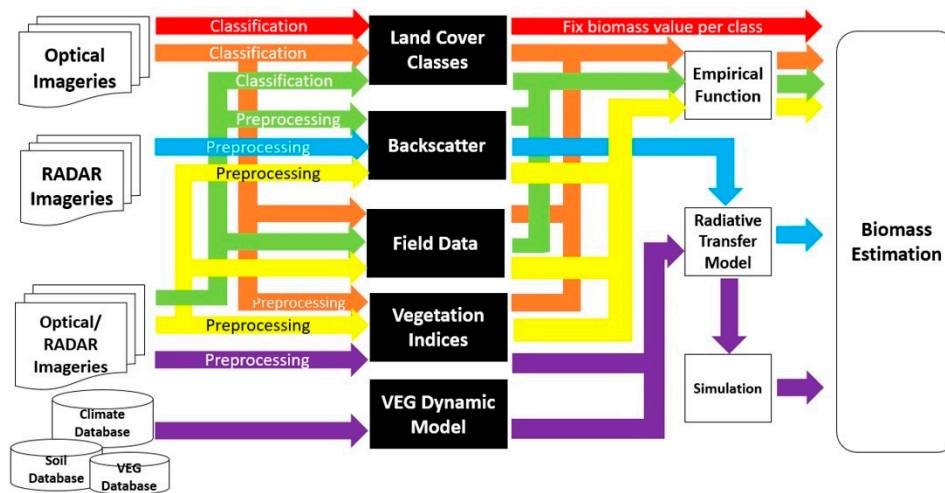


Figure 6. Different RS/GIS inputs and procedures available for estimating AGB. The figure is modified after [101].

5. Biophysical Predictors

The biophysical predictors of the vegetation growth need to be considered in RS studies due to the different rates of growth of various part of vegetation [109]. These predictors can be detected by remote sensors and are manifested through shadow, roughness, and spectral response [110]. RS variables measured and correlated with biomass quantification include the spectral reflectance of vegetation as the spectral properties of AGB obtained by the sensors have unique signature correlated with chlorophyll content in the plants [30]. The signals are sensitive to AGB structure and influenced by density, shadow, texture, soil moisture and roughness [101]. RS variables are correlated to the biophysical predictors in order to estimate AGB and the total biomass. The biophysical predictors used for estimating biomass include leaf area index (LAI), chlorophyll content, leaf nutrient concentration, crown measurements (crown area and crown diameter (CD)), height, DBH, stand basal area and greenness of canopy. All of these predictors are traditionally used to estimate biomass, but only some are applicable for RS based estimation (Figure 7).

Xiaoming et al. [111] observed a robust logarithmic correlation between LAI and AGB. LAI can be defined as the area of one-sided leaf tissue per unit ground and measures the density of the leaves surface in a canopy. Ten et al. [112] estimated LAI of oil palm in Malaysia using UK-DMC2 and ALOS POLSAR. They concluded that an increase in the LAI shows a proportional increase in the spectral reflectivity or Normalized Difference Vegetation Index (NDVI) during the initial growth stage; however, it presents little to no increase once it attains the full canopy cover due to sensor saturation. The ability of hyperspectral RS to collect reflectance in many narrow bands makes it particularly useful for extracting vegetation parameters, such as LAI, chlorophyll content, and leaf nutrient concentration [113]. Large scale photographs have been used to measure various forest characteristics, such as tree height, CD, crown closure, and stand area [81]. In their study on the indirect estimation of biomass, Popescu et al. [84] used RS data to determine tree canopy parameters, such as CD, using multiple regression analysis and canopy reflectance models. The area of the crown can be measured by satellite imagery and, thus, provide biomass estimation. Suganum et al. [114] found

that medium-resolution or more detailed spatial resolution data could be used for the crown coverage. Crown projection area (CPA), which is the canopy area that is covered by an individual tree, can be calculated by delineating trees using object-based image analysis [109,110]. Greenberg et al. [115] have effectively used IKONOS data (spatial resolution 4 m) for estimating crown projected area, DBH and stem density. Song et al. [85] estimated tree crown size from IKONOS and Quickbird images and concluded that this approach could provide estimates of average tree crown size for hardwood stands.

Height information of a tree can be retrieved using various approaches of RS, e.g., LiDAR and Radar. Height has been shown to be a potentially successful indicator for age in oil palms, for example, and it is widely used in estimating forest biomass [109]. Radar backscatters (P and L bands) are positively correlated not only with tree height and age but also with other major biophysical forest parameters such as DBH, basal area, and total AGB [22]. LiDAR sensor can directly measure three-dimensional (3D) components of vegetation canopy structure and is widely used in the estimation of forest biophysical parameters. LiDAR data are used for biomass estimation for different forest environments: tropical forest biomass, temperate mixed deciduous forest biomass, and in measurements of biophysical parameters such as tree height and stand volume, tree and CD, and canopy structure. The two-dimensional data (2D) have limitations in estimating vertical vegetation structures such as canopy height, which is one of the critical biophysical parameters for biomass estimation. Recently, optical data such as ALOS, panchromatic RS instrument for stereo mapping (PRISM), IKONOS stereo satellite images, and SPOT have been used to provide a stereo viewing capability that can be used to develop vegetation canopy height, thus improving biomass estimation performance [116]. St-Onge et al. [116] assessed the accuracy of the forest height and biomass estimates derived from an IKONOS stereo pair and a LiDAR digital terrain model. Reinartz et al. [117] used SPOT 5 HRS for forest height estimations in Bavaria and Spain, while Wallerman et al. [118] investigated 3-D information derived from SPOT 5 stereo imagery to map forest variables such as tree height, stem diameter and volume.

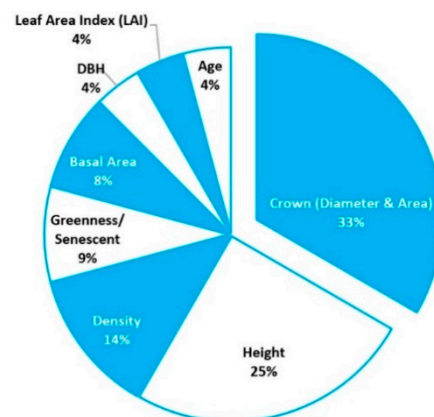


Figure 7. Percentages of different biophysical predictors used in RS-based methods.

6. Remote Sensing Variables

Vegetation index models are generally used to estimate biomass in many studies [98] (Figure 8). VIs are calculated from mathematical transformations of the original spectral reflectance data and can be used to interpret land vegetation cover [119]. VIs are applied to remove the variations caused by spectral reflectance measurements while also measuring the biophysical properties that result from the soil background, sun view angles, and atmospheric conditions [30]. The notion of VI is well adapted for quantifying vegetation over large areas, for example, over areas covering many pixels of an image [120]. VIs are quantitative measurements indicating the vigor of vegetation. They show better sensitivity for the detection of biomass than individual spectral bands [120]. Previous studies have shown a significant positive relationship between biomass and VIs [121]. In order to examine the relationship between AGB and RS variables including individual band reflectance values and VIs, Günlü et al. [122]

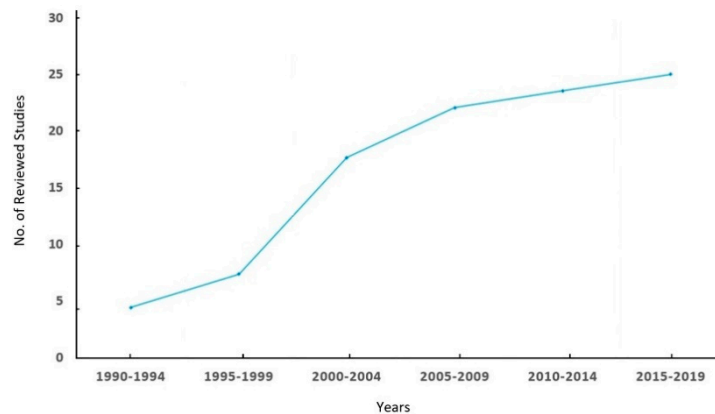
used Landsat TM in their study and found that VIs present better estimation of AGB in Anatolian pine forests with R^2 equal to 0.606, compared to individual band reflectance with R^2 of 0.465.

AGB models could be developed using many available predictors, grouped into two distinct categories: raw bands of the sensor as reflectance and VIs, including the simple ratio (SR), difference vegetation index (DVI), NDVI, ratio vegetation index (RVI), global environmental monitoring index (GEMI), soil adjusted vegetation index (SAVI), enhanced vegetation index (EVI), tasseled cap index of greenness (TCG), tasseled cap index of brightness (TCB), tasseled cap index of wetness (TCW), and many others. All these indices can measure the presence and density of green vegetation, overall reflectance (e.g., differentiating light from dark soils), soil moisture content, and vegetation density (structure). Most VIs rely on red and IR bands, which are the raw bands present in earth observation satellites and often contain more than 90% of the information related to vegetation [123–128]. Early studies have shown that both the simple ratio (NIR/Red) and the NDVI were closely related to dry matter accumulation [124]. The use of vegetation and other indices (e.g., NDVI, EVI, SAVI) are considered as part of the classification method. The principle of applying NDVI, for example in vegetation mapping, is that vegetation is highly reflective in the near infrared and highly absorptive in the visible red. The contrast between these channels can be used as an indicator of the vegetation status [78]. Sonnenschein et al. [129] used NDVI, SAVI and TCG from Landsat imageries for forests mapping in Greece. In a study conducted in Saudi Arabia, Aly et al. [130] found that NDVI images of Landsat could be classified into three classes of vegetation cover in arid regions, namely dense vegetation cover ($NDVI > 0.5$), moderate vegetation cover ($NDVI 0.25-0.5$), and sparse vegetation cover ($NDVI < 0.25$).

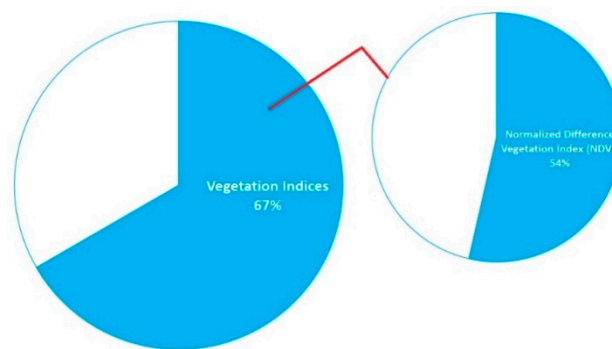
The ability of VIs to separate the vegetation from its background varies from one ecoregion to another, and from one plant species to another. VIs commonly used to estimate biophysical variables such LAI, APAR and biomass include NDVI, EVI, and SAVI [22]. NDVI is a prominent and frequently used index with different spatial resolutions of the optical sensors (Figure 8). Thenkabail et al. [63] implemented a regression model using NDVI and optical band reflectance 3 and 4 of IKONOS for estimation of AGB for oil palm in Africa, with 64–72% accuracy. Morel et al. [105] found that the Normalized Difference Fraction Index (NDFI) of Landsat ETM+ data performs better when estimating AGB for oil palm in Malaysia with R-value equal to 0.8. Srestasathiern and Rakwatin [131] found that the best performing VI to separate oil palms from its background was the Normalized Difference Index (NDI), which is a normalized ratio of green to the red band, and displays the highest discriminating power using a histogram dissimilarity metrics. Nevertheless, these results could not be generalized as all VIs must be tested. Zhao et al. [132] examined specific spectral bands of Landsat and their relationships with AGB in the Zhejiang province of Eastern China. They found that, when the forest stand structure is complex, VIs including shortwave infrared spectral bands (SWIR) had a higher correlation with AGB than others. However, the VIs including near-infrared wavelength (NIR) improved correlations with AGB in relatively simple forest stand structures. VIs can maximize the sensitivity for recording the green vegetation situation [122]. The choice of adequately performing VIs depends on the type of ecosystem, the environmental conditions and the spectral information available. In their study on forests in Bogotá, Colombia, Clerici et al. [10] estimated AGB and found that the best performing AGB estimation model was based on the RVI, with R^2 equal to 0.582. They also found that atmospheric and topographic correction was vital in improving model fit, especially in high aerosol and rugged terrain.

However, some studies had shown poor relationship between biomass and VIs compared with using raw bands [133]. Singh et al. [134] used two optical sensors (Landsat TM and SPOT 5) to assess their efficacy and evaluate disparities in forest composition and AGB in Sabah, Malaysia. They found that NDVI derived from SPOT 5 could distinguish between pristine forests and oil palm plantations. In fact, the reflectance values of bands 3 (red sensitive) and 4 (near infrared sensitive) of Landsat were strongly correlated with the field-based AGB values while both VIs derived from Landsat TM and SPOT 5 (such as NDVI) were weakly correlated with the field-based AGB values. The data saturation problem in Landsat imagery is well recognized and is regarded as an important factor resulting in

inaccurate forest AGB estimation, especially when AGB is high ($>130 \text{ Mg}\cdot\text{ha}^{-1}$) and when the forest structure is heterogeneous [132]. In a study to estimate total living biomass of Miombo woodlands of Tanzania, Gizachew et al. [135] found no clear evidence of data spectral saturation at higher biomass value in open canopy woodlands. They suggested that Landsat 8 OLI derived NDVI could be used as suitable auxiliary information for carbon monitoring in the context of the REDD+ program.



(a)



(b)

Figure 8. (a) Trend in vegetation indices use to derive AGB; (b) The Normalized Difference Vegetation Index (NDVI) percentage.

7. RS-GIS Integrated Models

GIS is usually employed to process model inputs and to visualize results [70]. However, building GIS-based models to predict future scenarios for forest management and the implementation of afforestation plans is another, more valuable product. In RS-GIS integrated models, RS data are used as input to the GIS model; where GIS act as a platform for data layering and database building in order to perform spatial data analysis and map creation. This not only saves time, but also allows for faster and better communication between research centers across the globe [70]. The use of geo-spatial modeling to study the current state of carbon sequestration and its future dynamics is a promising technique; it has the potential ability to tackle the ecological assessment problems [136]. Furthermore, as mentioned above, the integration of RS data into GIS models enables adding ancillary and field data (soil, climate, topography, etc.), in the analysis and increasing reliability in estimating AGB. For example, there are different GIS-based AGB estimation models that integrate other data models such as: digital terrain model (DTM), rainfall models, canopy height models, atmospheric scattering models, biomass production models, grazing models, 3D forest structure models and regression models [70,115,137–149]. An integrated classification approach, coupled with GIS analysis, has been employed successfully to improve land use and land cover (LULC), forest, and biomass mapping for

Landsat data [71]. Results show that an integration of RS and spatial analysis functions in GIS can increase the overall classification accuracy from 50.12% to 74.38% [93]. Furthermore, the integration of more than one sensor and the introduction of GIS-based models are becoming more common, used in around 12.3% and 12.8% of the reviewed studies, respectively. Indeed, we found more than 46 studies that used these two approaches together [150].

8. Arid Lands Case Studies with Challenges and Opportunities

Arid lands, defined as regions where annual potential evapotranspiration substantially exceeds precipitation, are critically important to society, yet exceptionally vulnerable to climate change [151]. Arid lands make up to 40% of the Earth's land surface and provide ecosystem services to more than two billion people, including supporting significant crop production and forage for wildlife and domestic livestock [3].

RS images can reduce the complexity of fieldwork by collecting quantitative and qualitative information at regular intervals and enabling the mapping of inaccessible places, as is the case in most arid regions [140,142,152–166]. In their review, Eisfelder et al. [101] stated that RS studies of vegetation in arid regions are scarce, and additional methodological research is needed to address the specific challenges faced by RS techniques in these environments. In our review, out of the 156 reviewed studies conducted from 1984 to 2019 to estimate AGB, only 12 studies were conducted in arid lands and another 21 studies in semiarid ecosystems (more than a third of these studies were conducted in Niger and Senegal). Figure 9 shows the proportions of RS-based AGB estimation studies in arid and semi-arid regions taking into account the proportion of reviewed studies, sensors used and their spatial resolutions, the use of GIS tools and locations of the studies (Figure 9).

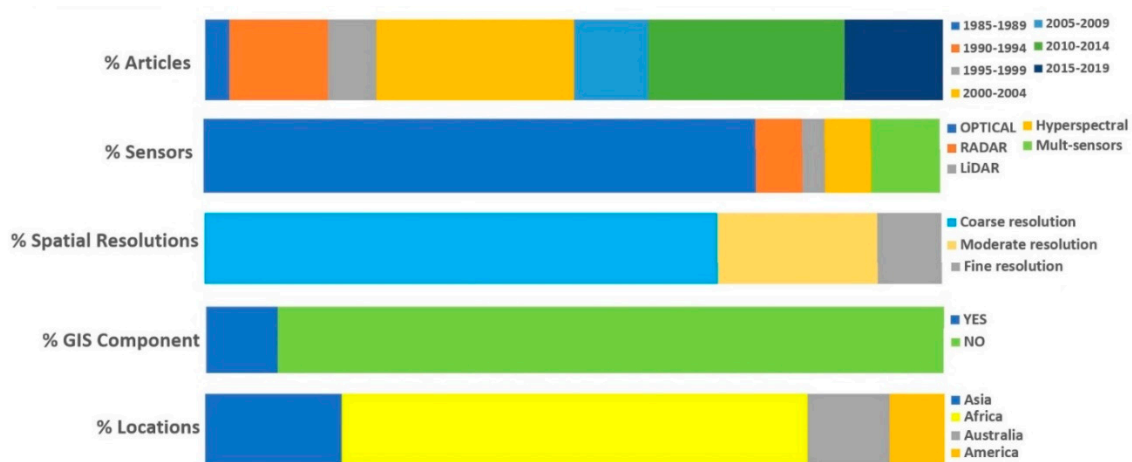


Figure 9. Summary of published studies on estimating AGB using geo-spatial technologies in arid and semi-arid ecosystems during the last two decades.

As mentioned above, monitoring the spatiotemporal dynamics of arid lands ecosystem structure and function is therefore a high research priority. Although the methods detailing vegetation cover mapping and estimation integrating RS and GIS are well developed, research on RS-based biomass estimation for arid lands is relatively scarce compared to other ecosystems (tropical, subtropical, temperate and boreal forests) [101]. Very few biomass measurements are available for plant species in desert ecosystems. Although biomass per unit area is normally low in those regions, the vast extent of the Earth's arid lands gives it a significant role as a carbon pool and for the supply of essential ecosystem services [167]. Studies showed a strong link between desertification and emission of CO₂ from soil and vegetation to the atmosphere [168]. Desertification, and degradation of soils and vegetation in arid lands resulting from climatic and anthropogenic factors, affects more than one billion hectares of soils and more than 2.5 billion hectares of rangelands globally. Furthermore, an alarming estimate of six

billion hectares of land is affected by desertification per year [168]. Lal [168] in his study, concluded that the total world historic loss of carbon due to desertification in the period between 1850 and 1998 was in the order of 19–29 Pg, an amount that could have been sequestered. Information on biomass helps to quantify the resilience of arid land systems and is thus essential for sustainable land-use management [146]. Hence, suitable methods to map biomass in arid land regions still need to be developed [163].

If plant species are very scattered, which is the case for most arid lands ecosystems, where vegetation is characterized by its patchiness pattern, the background reflection is mostly related to the soil. Hence, the selection of sites must be characterized by their relatively high density of plant species under study in order to reduce the background effects as much as possible. In addition, the selected sites must be relatively large in area and be homogenous, to enable the extraction of real spectral signature that represent the species to be mapped or to use a minimum number of field plots within each pixel as well as to increase the spatial/spectral resolution of the sensors used [101].

Moreover, using satellite images to map and correlate biomass is only possible if the target vegetation spectra are strong enough to be identified within the pixel [130,169,170]. This presents a major challenge in the desert where vegetation is usually sparse, offering a small spectral target that requires higher resolutions to be detected [171]. In the desert environment in China, Ren et al. [162] estimated crop biomass of individual components (e.g., leaves, stems) for the whole season using red edge reflectance of hyperspectral data. Optical RS probably provides the best alternative to biomass estimation using remote sensors due to its historic global coverage, repetitiveness and cost-effectiveness and thus is useful and operational in dry lands. Such regions can be found in most of the low-income developing or least developed countries. Zandler et al. [167] used Landsat 8 OLI in the arid regions of Tajikistan to model total biomass in extremely low vegetation cover. The coverage of the SWIR spectral region showed the importance in detecting shrubs or nonphotosynthetic vegetation. To deal with soil brightness, the study used additional soil adjusted VIs variations such as SAVI, transformed soil-adjusted vegetation index (TSAVI), and modified soil-adjusted vegetation index (MSAVI) as VIs suffer from various soil effects, especially when vegetation cover is low. The study indicated that biomass quantification in this arid setting is feasible but is subject to large uncertainties. One of the main challenges is the extreme aridity and the associated strong influence of soil background. Another challenge is the fact that large parts of arid or desert plants consist of nonphotosynthetic, woody matter and hence the photosynthetic signal, captured by most spectral bands and indices, may be low in relation to the biomass amount.

In order to overcome the limitations of current remote sensing techniques, especially in arid lands, we recommend: (1) Exploring novel combinations of sensors and techniques (e.g., solar-induced fluorescence, thermal, microwave, hyperspectral, and LiDAR) across a range of spatiotemporal scales to gain new insights into arid land ecosystems' dynamics; (2) utilizing near-continuous observations from new-and-improved satellites to capture the subtle variations of arid land ecosystems; (3) developing algorithms that are specifically designed to meet arid land ecosystems conditions and coupling remote sensing observations with process-based models to improve our understanding of the arid land ecosystem dynamics and for long-term projections.

9. Merits, Gaps, Limitations and Accuracy of the Geo-Spatial Methods

Although RS has proven to be efficient in saving time and money, this technology cannot achieve its goal without additional field and data measurements [13]. Nevertheless, the amount of fieldwork required when using RS is significantly reduced. This should not lead to the rejection of the traditional methods for AGB estimation, but allow instead for using the advantages of geo-spatial technologies methods to accelerate and enhance existing methods through process integration and modeling [88]. Geo-spatial technologies can be a modern alternative to traditional methods in estimating AGB and will continue to be further developed; however, they do not come without their limitations and drawbacks. Despite the successful application of various sensors in AGB estimation, there are challenges related to

acquisition costs, area coverage (swath width), and limited availability. Selecting the “right” sensor is associated with the specific data availability of the area under study, project budget, technical skill requirements for data interpretation, and software packages. Table 4 summarizes the main limitations and benefits of using different sensors in AGB estimation studies. The technology used in RS includes satellites, aerial photography devices such as drones, computers and sensors which are all extremely costly. The maintenance of this technology can also be costly, requiring specialized care and trained professionals. Using computers to analyze the incoming data requires training and skills, such as being able to read the GIS maps and make sense of the incoming RS imagery. The training of the scientists involved in this discipline can be costly. Furthermore, with the constant development of technology, the knowledge in applied remote sensing will continue to develop. This translates to GIS and RS specialists needing to continually acquire the latest training and skills [172].

The optical imagery-based technologies are commonly used for biomass estimation due to high correlations between spectral bands and biomass [132]. On the other hand, Carson et al. [173] found that the Landsat TM and SPOT data with a ground resolution of 30 and 20 m, respectively, are not considered useful for mapping at the species level unless the stand of an invasive species is large enough. Due to the limitation of spatial resolution, Landsat products are usually used to map vegetation at the community level. Using Landsat images for mapping at the species level is challenging, especially in a heterogeneous environment. Although VIs, especially derived NDVI, can distinguish among different vegetation, some studies found that the spectral variables were limited in their effectiveness in differentiating between forest types, and in estimating their biomass. Spectrally, NDVI saturation could lead to the underestimation of biomass carbon in certain places. In a study to derive spectrally modeled AGB of coniferous forests of Western Himalaya, Wani et al. [96] attributed the underestimation of biomass to the shadow effect resulting in decreased overall reflectance. Conversely, they referred the overestimation of biomass in other locations of their study area to the mixing up of reflectance contributed by soil and crown cover, leading to an increase in overall reflectance [96].

When using RS in ecological subjects such as assessing carbon stock, uncertainties are high due to vegetation structural variations, heterogeneity of landscapes, species composition, soil properties, climatic variables and seasonality, topographical variables, disproportionate data availability and human activities. These uncertainties can have a great impact on biomass distribution and change tendency [11,25,69,107]. Also, no RS sensor can measure forest carbon stock directly without additional ground-based collection [18]. One of the widespread limitations of the vegetation mapping is that the same vegetation type on the ground may have different spectral features in remotely sensed images. Further, different vegetation types may possess similar spectra, which makes it very hard to obtain accurate classification results. It is important to consider the biological traits of plants in order to distinguish these from their surroundings and other vegetation covers. Characteristics of these biological traits include (1) peak flowering, which is critical for timing imagery acquisition, (2) plant pubescence, which affects the reflectance of visible light and infrared (early green-up or late senescence), and (3) canopy architecture, which affects the brightness and darkness of image response. Plants with biological characteristics that are readily distinguishable spectrally from the surrounding vegetation can be detected by lower spectral resolution imagery. Forest biomass is continuously affected by disturbance [174]; likewise, forest structure is also influenced by environmental conditions, ecological processes of tree growth, mortality, and decomposition [76]. Comprehensive time-series records are required to accurately monitor forest change in dynamic systems [175]. All these issues must be considered when applying RS change detections studies.

Table 4. A summary of limitations and benefits of Optical, RADAR, and LiDAR sensors used for estimating the Above Ground Biomass (AGB) of standing forests.

Sensor Types	Approaches/Resolutions	Limitations	Benefits
Optical Sensors	<i>Coarse Resolution Spatial</i> (>100 m) Examples: MODIS, AVHRR, NOAA, METEOSAT and SPOT Vegetation	Average R value of 0.58, with average predictive of 42% Saturation of spectral data at high biomass density Mismatch between the size of field plots, field measurements and pixel size (mixed pixels) Cloud cover Limited to discriminating vegetation structure	Availability of data with huge datasets archived Estimation and mapping of AGB at continental and global scale Repetitive, with high temporal frequency increasing the probability of acquiring cloud-free data Provide consistent spatial data
	<i>Medium Spatial Resolution</i> (10–100 m) Examples: TM Landsat, ETM+, OLI and SPOT	Average R value of 0.68 with average predictive error of 32% Single pixel can encompass many tree crown or noncrown features No reliable indicators of biomass in closed canopy structure Not all texture measures can effectively extract biomass information	Provide consistent global data Archived datasets back to 1972 for Landsat Small to large-scale mapping Cost-effective (Free)
	<i>Fine Spatial Resolution</i> (<5 m) Examples: Quickbird, WorldView-2, and IKONOS	Need large data storage and processing time High cost, and more costly when it applies on large areas	Average R value of 0.75 and average predictive error (27%) Estimate tree crown size Validation at localized scale
	<i>Hyperspectral</i> Many, very narrow, and contiguous spectral bands Examples: AISA Eagle, HYDICE and ALOS	Cloud cover High cost Suffers from band redundancy and saturation in dense canopy Computationally intensive and technically demanding	Average R value of 0.83 Allows discrimination of subtler differences (species level) Potential for the future of RS-based biomass estimation models Integration with LiDAR can improve results.
		Not accurate in mountainous region due to spurious relation between AGB and backscatter values. Signal saturation in mature forests at various wavelengths (C, L and P bands) Polarization (e.g., HV and VV) problems Low spatial resolution makes it inaccurate for AGB assessment at the species level. Cannot be applied on any vegetation type without considering stand characteristics and ground conditions.	Measure forest vertical structure Generally free Can be accurate for young and sparse forests Repetitive data Can give an average R value of 0.74, with average predictive error of 25%. Integrating RADAR with multi source data (optical, microwave data and GIS modeling techniques) is a promising approach.
RADAR Sensors	Approaches involve the use of either backscatter values or interferometry techniques Examples: Microwave/radar i.e., ALOS PALSAR, ERS-1, Envisat and JERS-1.		
LiDAR Sensors	Using laser light Spatial Resolution: (0.5 cm–5 m) Examples: Carbon 3D	Repetitive at high cost and logistics deployment Requires extensive field data calibration Highly expensive Technically demanding	Penetrate cloud cover and canopy Among all sensors option, LiDAR is the easiest to use for the extraction of tree attributes for estimating AGB with great accuracy Accurate for estimating forest biomass in all spatial variability (sparse, young or mature forests) - Average R value of 0.89, with average predictive error equal 14% - Potential for satellite-based system to estimate global forest carbon stock

Accuracy of predictions is often assessed using independent field plots or Lidar-based AGB data. It is important to note that uncertainties arising from ingesting different data sources need

to be carefully considered given the inconsistency in inventory methods including plot sizes and survey techniques [176]. There are many limitations associated with low spatial resolutions data (>80 m). One of these limitations is the mismatch between the size of field plot and pixel size producing poor prediction's accuracy of AGB due to mixed pixels [22,30]. This limitation is lowering the average of determination coefficient (R^2 value) to be 0.58, with an average predictive error equal to 42% [177]. With moderate optical resolution data (10–80 m), the accuracy of estimation of AGB is improved, averaging an R^2 value of 0.68 and an average predictive error of AGB estimation of 32% [177]. The popularity of multispectral sensors urged researchers on AGB studies to apply advanced techniques (such as pan sharpening or multiresolution merging) in order to improve the accuracy of their estimates for large areas [178,179]. An example was the combination of medium resolution Landsat TM data with AVHRR coarse resolution data in the boreal forests of Finland and Norway along with different modeling approaches, which provided more accurate biomass estimation for large areas as done by Hame et al. [180]. With fine spatial resolution data (<10 m), we can estimate the forests biophysical variables such as tree crown size which is essential in running the allometric equations with high precision and accuracy order. Hence, by using fine spatial resolution data, the average R^2 value can reach 0.75 with an average predictive error equal to 27% [177]. Furthermore, with high spectral resolution data such as the hyperspectral sensors' data, the average R^2 value in estimating AGB can reach high levels of accuracy especially in desert and arid lands.

Both multispectral and hyperspectral sensors have been used in AGB studies however, and despite accuracy problems and limited numbers of spectral bands, multispectral optical sensors have been more frequently utilized operationally in estimating and mapping AGB [18,22,25,45,88,101]. AGB estimation in western China showed that integrating SPOT5 data with LiDAR could increase biomass estimation accuracy ($R^2 = 0.784$) [181]. Basuki et al. [182] likewise, integrating RADAR with optical sensors can reduce both the mixed pixels and the saturation problems. For example, combining ETM+ data with RADAR data in estimating the biomass of tropical forests in Indonesia achieved an R^2 value ranging between 0.7 and 0.75.

In respect of the limitations and gaps summarized above, we propose a framework combining multiscale RS techniques and building on the previously established and growing ground observation stations especially in arid lands:

- Measuring other plants' variables rather than limiting our research to VIs. As these indices suffer from several weaknesses in arid lands ecosystems, as explained above.
- Measuring vegetation optical depth (VOD) using microwave sensors to assess vegetation water content [183] and relates closely with total AGB [184].
- Measuring chlorophyll fluorescence (ChlF) (which is the re-emittance of excess energy by the photosystems during the light reactions of photosynthesis [185]. This is highly related to total AGB,
- Measuring land surface temperature (LST) from the Thermal infrared (TIR) band, which can be integrated with measurements of air temperature to infer rates of canopy transpiration [186,187],
- Finally, hyperspectral imaging spectroscopy can provide more information relative to traditional multispectral platforms. A single full-range hyperspectral reflectance spectrum (400–2500 nm) can provide information on a variety of functional traits, including vegetation water, nitrogen, chlorophyll, carotenoid, and xanthophyll dynamics [188–190] that can be used to map functional traits and life history strategies across the landscape [190].

10. Conclusions–Recommendations and Future Works

The conclusions of our review are consistent with the consensus of numerous scientific papers on the subject published in the last five decades. Geo-spatial technologies are practical, feasible and provide an adequate validation for AGB assessment monitoring, modeling and management of carbon sequestration. The use of these technologies can provide a useful tool, especially for developing countries, for measuring, mapping, monitoring, modeling and management of their carbon stock in

biomass and soil; leading to improve soil and plant productivity, to increase food security, and to control land degradation. In their turn, these countries can play a significant role in reducing the negative impacts of climate change, by mitigating carbon emissions.

There are many methods that could be used for estimating carbon stock, and all of them have their advantages and disadvantages. Traditional methods relying on heavy fieldwork measurements are the most accurate, but they require significant time, expense and labor, and can be damaging for the ecosystems. Building allometric equations can help avoid the destructive nature and other disadvantages of the fieldwork method. However, most of the allometric equations are mixed species equations and not tailored for single species; most of them are also built for specific sites and ecosystems (less applicable for arid regions). Also, it is recommended building the allometric biomass equations using variables that rely more on RS techniques to estimate biomass and carbon stock (crown and height attributes). Building a database including the rates of carbon sequestered and stored for each plant species, especially those with high economic values, will fill the gap and increase our understanding of the atmospheric carbon sequestration potential of plant species and ecosystems.

Solely using RS may not always be possible as ground measurements, such as soil samples and verification of results by ground truthing are required at some stages in the estimation of biomass. The best fit methodology relies on both fieldwork and the analysis of RS data. The suggested process involves three steps, including: pre-field preparations to identify sample areas of interest, fieldwork that includes sample collection and measurement of plant characteristics, and post-field activity that focuses on processing RS data, classification, model development and validation. Assessing carbon stocks remotely and consistently over large areas varies greatly depending on the type of instruments used, and the platforms. Nevertheless, these difficulties could be solved and tackled using different sensor options and other innovative methods, and hence avoiding the limitations that relate to aspects such as scale, cost, and associated errors and uncertainties.

High resolution RS data are the most accurate. However, moderate resolution satellite data, such as Landsat, have shown to be effective in estimating AGB and, consequently, carbon stock, with good accuracy. Furthermore, these sensors provide invaluable historical data to monitor the change of carbon stock over time. Developing algorithms that combine more than one remote sensor is highly important for tackling the challenges associated with estimating AGB and subsequently assessing carbon sequestration. Merging and fusion of more than one set of data have the potential to reduce uncertainty errors in biomass estimation. In such studies, it is important to consider the effects of bioclimatic factors depending on parameters such as plant age, species, forest type, rainfall, topography, vegetation structural variations, heterogeneity of landscapes, and seasonality. One of the common challenges in achieving this, is mapping the spatial patterns of vegetation and soil carbon and producing geo-referenced estimates of carbon. Such maps provide a better understanding of carbon dynamics and help quantify the regional and global carbon budgets. In addition, this will provide decision makers with a strong knowledge base to be able to identify and focus on the most essential issues.

We argue that arid lands RS research should be a high research priority, especially given that more than 2 billion people depend on services provided by arid lands ecosystems. Hereafter, we offer a framework by which current and coming RS activities could be optimally utilized to accelerate our knowledge of arid land ecosystem dynamics, by adopting some emerging new techniques such as: (i) Measuring other plants' variables rather than limiting our research to VIs.; (ii) Measuring vegetation optical depth (VOD); (iii) Measuring chlorophyll fluorescence (ChlF); (iv) Measuring land surface temperature (LST) from the Thermal infrared (TIR) bands and; (v) Finally, hyperspectral imaging spectroscopy can provide more information relative to traditional multispectral platforms.

A combination of the field-based measurements and geo-spatial approaches reviewed in this paper have the potential to help improve carbon estimation to reduce emissions resulting from deforestation and forest degradation (REDD+), and to design incentive programs in the countries with arid land regions. A renewed prioritization of arid lands remote sensing is needed, especially given rapidly

developing field-based remote sensing techniques and the upcoming diversity of observations that will be available from space. In order to exploit these new opportunities, the following research areas should be emphasized: (1) Exploring novel combinations of sensors and techniques (e.g., solar-induced fluorescence, thermal, microwave, hyperspectral, and LiDAR) across a range of spatiotemporal scales to gain new insights into arid lands ecosystems' dynamics; (2) Utilizing near-continuous observations from new-and-improved satellites to capture the subtle variations of arid lands ecosystems; (3) Developing algorithms that are specifically designed to meet arid lands ecosystems conditions and coupling remote sensing observations with process-based models to improve our understanding of the arid lands ecosystem dynamics and for long-term projections.

Author Contributions: S.I. envisioned, designed this research and wrote the paper; B.D. processed the data, interpreted the results and participated in writing the paper; T.K. conceptualized and reviewed the paper; N.S. helped to review the writing and giving comments. All authors have read and agreed to the published version of the manuscript.

Funding: This research has been funded by the United Arab Emirates University—Research Affaires, under the UPAR grant program. Fund No 31S247.

Conflicts of Interest: The authors declare no conflict of interest.

References

1. Lackner, K.S. A guide to CO₂ sequestration. *Science* **2003**, *300*, 1677–1678. [[CrossRef](#)] [[PubMed](#)]
2. Brown, S. *Estimating Biomass and Biomass Change of Tropical Forests: A Primer*; Food & Agriculture Organization: Rome, Italy, 1997; Volume 134.
3. Bestelmeyer, B.T.; Okin, G.S.; Duniway, M.C.; Archer, S.R.; Sayre, N.F.; Williamson, J.C.; Herrick, J.E. Desertification, land use, and the transformation of global drylands. *Front. Ecol. Environ.* **2015**, *13*, 28–36. [[CrossRef](#)]
4. Ahlström, A.; Raupach, M.R.; Schurgers, G.; Smith, B.; Arneeth, A.; Jung, M.; Reichstein, M.; Canadell, J.G.; Friedlingstein, P.; Jain, A.K. The dominant role of semi-arid ecosystems in the trend and variability of the land CO₂ sink. *Science* **2015**, *348*, 895–899. [[CrossRef](#)] [[PubMed](#)]
5. Biederman, J.A.; Scott, R.L.; Bell, T.W.; Bowling, D.R.; Dore, S.; Garatuza-Payan, J.; Kolb, T.E.; Krishnan, P.; Krofcheck, D.J.; Litvak, M.E. CO₂ exchange and evapotranspiration across dryland ecosystems of southwestern North America. *Glob. Chang. Biol.* **2017**, *23*, 4204–4221. [[CrossRef](#)]
6. Humphrey, V.; Zscheischler, J.; Ciais, P.; Gudmundsson, L.; Sitch, S.; Seneviratne, S.I. Sensitivity of atmospheric CO₂ growth rate to observed changes in terrestrial water storage. *Nature* **2018**, *560*, 628–631. [[CrossRef](#)]
7. Poulter, B.; Frank, D.; Ciais, P.; Myneni, R.B.; Andela, N.; Bi, J.; Broquet, G.; Canadell, J.G.; Chevallier, F.; Liu, Y.Y. Contribution of semi-arid ecosystems to interannual variability of the global carbon cycle. *Nature* **2014**, *509*, 600–603. [[CrossRef](#)]
8. Qureshi, A.; Badola, R.; Hussain, S.A. A review of protocols used for assessment of carbon stock in forested landscapes. *Environ. Sci. Policy* **2012**, *16*, 81–89. [[CrossRef](#)]
9. Vicharnakorn, P.; Shrestha, R.P.; Nagai, M.; Salam, A.P.; Kiratiprayoon, S. Carbon stock assessment using remote sensing and forest inventory data in Savannakhet, Lao PDR. *Remote Sens.* **2014**, *6*, 5452–5479. [[CrossRef](#)]
10. Clerici, N.; Rubiano, K.; Abd-Elrahman, A.; Posada Hoestettler, J.M.; Escobedo, F.J. Estimating aboveground biomass and carbon stocks in periurban Andean secondary forests using very high resolution imagery. *Forests* **2016**, *7*, 138. [[CrossRef](#)]
11. Corona-Núñez, R.O.; Campo, J.; Williams, M. Aboveground carbon storage in tropical dry forest plots in Oaxaca, Mexico. *For. Ecol. Manag.* **2018**, *409*, 202–214. [[CrossRef](#)]
12. United Nation the Kyoto Protocol—Status of Ratification|UNFCCC. Available online: <https://unfccc.int/process/the-kyoto-protocol/status-of-ratification> (accessed on 25 December 2019).
13. Dick, O.B.; Wondrade, N. Estimating above Ground Biomass and Carbon Stock in the Lake Hawassa Watershed, Ethiopia by Integrating Remote Sensing and Allometric Equations. *For. Res. Open Access* **2015**, *4*. [[CrossRef](#)]

14. Ekoungoulou, R.; Liu, X.; Loumeto, J.J.; Ifo, S.A.; Bocko, Y.E.; Fleury, E.K.; Niu, S. Tree Allometry in Tropical Forest of Congo for Carbon Stocks Estimation in above-Ground Biomass. *Open J. For.* **2014**, *4*, 481. [[CrossRef](#)]
15. Singh, S.L.; Sahoo, U.K.; Kenye, A.; Gogoi, A. Assessment of Growth, Carbon Stock and Sequestration Potential of Oil Palm Plantations in Mizoram, Northeast India. *J. Environ. Prot.* **2018**, *9*, 912. [[CrossRef](#)]
16. Prayogo, C.; Sari, R.R.; Asmara, D.H.; Rahayu, S.; Hairiah, K. Allometric Equation for Pinang (*Areca catechu*) Biomass and C Stocks. *AGRIVITA J. Agric. Sci.* **2018**, *40*, 381–389. [[CrossRef](#)]
17. Khalid, N.; Hamid, J.R.A. Development of Allometric Equation for Estimating Aboveground Biomass in Ampang Forest Reserve, Malaysia. *J. Biodivers. Manag. For.* **2017**, *4*, 2. [[CrossRef](#)]
18. Gibbs, H.K.; Brown, S.; Niles, J.O.; Foley, J.A. Monitoring and estimating tropical forest carbon stocks: Making REDD a reality. *Environ. Res. Lett.* **2007**, *2*, 045023. [[CrossRef](#)]
19. Lal, R. Soil carbon sequestration to mitigate climate change. *Geoderma* **2004**, *123*, 1–22. [[CrossRef](#)]
20. Koala, J.; Sawadogo, L.; Savadogo, P.; Aynekulu, E.; Heiskanen, J.; Saïd, M. Allometric equations for below-ground biomass of four key woody species in West African savanna-woodlands. *Silva Fenn.* **2017**, *51*, 1631. [[CrossRef](#)]
21. Eggleston, H.S.; Buendia, L.; Miwa, K.; Ngara, T.; Tanabe, K. IPCC guidelines for national greenhouse gas inventories. *Inst. Glob. Environ. Strateg. Hayama Jpn.* **2006**, *2*, 48–56.
22. Kumar, L.; Sinha, P.; Taylor, S.; Alqurashi, A.F. Review of the use of remote sensing for biomass estimation to support renewable energy generation. *J. Appl. Remote Sens.* **2015**, *9*, 097696. [[CrossRef](#)]
23. Fonton, N.H.; Medjibé, V.; Djomo, A.; Kondaoulé, J.; Rossi, V.; Ngomanda, A.; Maidou, H. Analyzing accuracy of the power functions for modeling aboveground biomass rediction in Congo basin tropical forests. *Open J. For.* **2017**, *7*, 388–402.
24. Cairns, M.A.; Brown, S.; Helmer, E.H.; Baumgardner, G.A. Root biomass allocation in the world's upland forests. *Oecologia* **1997**, *111*, 1–11. [[CrossRef](#)] [[PubMed](#)]
25. Kumar, L.; Mutanga, O. Remote Sensing of above-Ground Biomass. *Remote Sens.* **2017**, *9*, 935. [[CrossRef](#)]
26. Joshi, H.G.; Ghose, M. Community structure, species diversity, and aboveground biomass of the Sundarbans mangrove swamps. *Trop. Ecol.* **2014**, *55*, 283–303.
27. Cihlar, J.; Denning, S.; Ahem, F.; Arino, O.; Belward, A.; Bretherton, F.; Cramer, W.; Dedieu, G.; Field, C.; Francey, R. Initiative to quantify terrestrial carbon sources and sinks. *Eos Trans. Am. Geophys. Union* **2002**, *83*, 1–7. [[CrossRef](#)]
28. Kankare, V.; Vastaranta, M.; Holopainen, M.; Rätty, M.; Yu, X.; Hyyppä, J.; Hyyppä, H.; Alho, P.; Viitala, R. Retrieval of forest aboveground biomass and stem volume with airborne scanning LiDAR. *Remote Sens.* **2013**, *5*, 2257–2274. [[CrossRef](#)]
29. Wannasiri, W.; Nagai, M.; Honda, K.; Santitamont, P.; Miphokasap, P. Extraction of mangrove biophysical parameters using airborne LiDAR. *Remote Sens.* **2013**, *5*, 1787–1808. [[CrossRef](#)]
30. Lu, D. The potential and challenge of remote sensing-based biomass estimation. *Int. J. Remote Sens.* **2006**, *27*, 1297–1328. [[CrossRef](#)]
31. Houghton, N.; Abramowitz, G.; De Kauwe, M.G.; Pitman, A.J. Does predictability of fluxes vary between FLUXNET sites? *Biogeosciences* **2018**, *15*, 4495–4513. [[CrossRef](#)]
32. Wu, X.B.; Archer, S.R. Scale-dependent influence of topography-based hydrologic features on patterns of woody plant encroachment in savanna landscapes. *Landsc. Ecol.* **2005**, *20*, 733–742. [[CrossRef](#)]
33. Cheng, T.; Song, R.; Li, D.; Zhou, K.; Zheng, H.; Yao, X.; Tian, Y.; Cao, W.; Zhu, Y. Spectroscopic Estimation of Biomass in Canopy Components of Paddy Rice Using Dry Matter and Chlorophyll Indices. *Remote Sens.* **2017**, *9*, 319. [[CrossRef](#)]
34. Yuen, J.Q.; Fung, T.; Ziegler, A.D. Review of allometric equations for major land covers in SE Asia: Uncertainty and implications for above-and below-ground carbon estimates. *For. Ecol. Manag.* **2016**, *360*, 323–340. [[CrossRef](#)]
35. Maulana, S.I.; Wibisono, Y.; Utomo, S. Development of local allometric equation to estimate total aboveground biomass in Papua tropical forest. *Indones. J. For. Res.* **2016**, *3*, 107–118. [[CrossRef](#)]
36. Mokany, K.; Raison, R.; Prokushkin, A.S. Critical analysis of root: Shoot ratios in terrestrial biomes. *Glob. Chang. Biol.* **2006**, *12*, 84–96. [[CrossRef](#)]
37. Ramankutty, N.; Gibbs, H.K.; Achard, F.; Defries, R.; Foley, J.A.; Houghton, R.A. Challenges to estimating carbon emissions from tropical deforestation. *Glob. Chang. Biol.* **2007**, *13*, 51–66. [[CrossRef](#)]
38. Houghton, R.A.; Hall, F.; Goetz, S.J. Importance of biomass in the global carbon cycle. *J. Geophys. Res. Biogeosciences* **2009**, *114*. [[CrossRef](#)]

39. Walkley, A.; Black, I.A. An examination of the Degtjareff method for determining soil organic matter, and a proposed modification of the chromic acid titration method. *Soil Sci.* **1934**, *37*, 29–38. [[CrossRef](#)]
40. Brady, N.C.; Weil, R.R. *The Nature and Properties of Soil*, 12th ed.; Prentice-Hall Inc.: Upper Saddle River, NJ, USA, 1999.
41. Pribyl, D.W. A critical review of the conventional SOC to SOM conversion factor. *Geoderma* **2010**, *156*, 75–83. [[CrossRef](#)]
42. Ponce-Hernandez, R.; Koohafkan, P.; Antoine, J. *Assessing Carbon Stocks and Modelling Win-Win Scenarios of Carbon Sequestration through Land-Use Changes*; Food & Agriculture Organization: Rome, Italy, 2004; Volume 1.
43. Picard, N.; Saint-André, L.; Henry, M. *Manual for Building Tree Volume and Biomass Allometric Equations: From Field Measurement to Prediction*; FAO: Rome, Italy, 2012.
44. Mahmood, H.; Siddique, M.R.; Costello, L.; Birigazzi, L.; Abdullah, S.R.; Henry, M.; Siddiqui, B.N.; Aziz, T.; Ali, S.; Al Mamun, A. Allometric models for estimating biomass, carbon and nutrient stock in the Sal zone of Bangladesh. *iFor. Biogeosci. For.* **2019**, *12*, 69. [[CrossRef](#)]
45. Vashum, K.T.; Jayakumar, S. Methods to estimate above-ground biomass and carbon stock in natural forests—A review. *J. Ecosyst. Ecogr.* **2012**, *2*, 1–7. [[CrossRef](#)]
46. Russell, C.E. *Nutrient Cycling and Productivity of Native and Plantation Forests at Jari Florestal, Para, Brazil*; University of Georgia: Athens, GA, USA, 1983.
47. Deans, J.D.; Moran, J.; Grace, J. Biomass relationships for tree species in regenerating semi-deciduous tropical moist forest in Cameroon. *For. Ecol. Manag.* **1996**, *88*, 215–225. [[CrossRef](#)]
48. Brown, I.F.; Martinelli, L.A.; Thomas, W.W.; Moreira, M.Z.; Ferreira, C.C.; Victoria, R.A. Uncertainty in the biomass of Amazonian forests: An example from Rondonia, Brazil. *For. Ecol. Manag.* **1995**, *75*, 175–189. [[CrossRef](#)]
49. Khalid, H.; Zin, Z.Z.; Anderson, J.M. Quantification of oil palm biomass and nutrient value in a mature plantation. I. Above-ground biomass. *J. Oil Palm Res.* **1999**, *11*, 23–32.
50. Duncanson, L.; Rourke, O.; Dubayah, R. Small sample sizes yield biased allometric equations in temperate forests. *Sci. Rep.* **2015**, *5*, 17153. [[CrossRef](#)]
51. Sileshi, G.W. A critical review of forest biomass estimation models, common mistakes and corrective measures. *For. Ecol. Manag.* **2014**, *329*, 237–254. [[CrossRef](#)]
52. Cheng, Z.; Gamarra, J.G.P.; Birigazzi, L. *Inventory of Allometric Equations for Estimation Tree Biomass—A Database for China*; UNREDD Programme: Rome, Italy, 2014.
53. Chave, J.; Andalo, C.; Brown, S.; Cairns, M.A.; Chambers, J.Q.; Eamus, D.; Fölster, H.; Fromard, F.; Higuchi, N.; Kira, T. Tree allometry and improved estimation of carbon stocks and balance in tropical forests. *Oecologia* **2005**, *145*, 87–99. [[CrossRef](#)]
54. Sajdak, M.; Velázquez-Martí, B.; López-Cortés, I. Quantitative and qualitative characteristics of biomass derived from pruning *Phoenix canariensis* hort. ex Chabaud. and *Phoenix dactylifera* L. *Renew. Energy* **2014**, *71*, 545–552. [[CrossRef](#)]
55. Sanquetta, C.R.; Péllico Netto, S.; Dalla Corte, A.P.; Lourenço, A. Quantifying biomass and carbon stocks in oil palm (*Elaeis guineensis* Jacq.) in Northeastern Brazil. *Afr. J. Agric. Res.* **2015**, *10*, 4067–4075.
56. Henson, I.E.; Chang, K.C. Oil palm plantations and forest loss an objective appraisal. In Proceedings of the PIPOC 2003 International Palm Oil Congress, Kuala Lumpur, Malaysia, 25–29 September 2003; pp. 960–974.
57. Issa, S.; Dahy, B.; Saleous, N.; Ksiksi, T. Carbon stock assessment of date palm using remote sensing coupled with field-based measurements in Abu Dhabi (United Arab Emirates). *Int. J. Remote Sens.* **2019**, *40*, 7561–7580. [[CrossRef](#)]
58. Issa, S.; Dahy, B.; Ksiksi, T.; Saleous, N. Development of a New Allometric Equation Correlated WITH RS Variables for the Assessment of Date Palm Biomass. In Proceedings of the 39th Asian Conference on Remote Sensing (ACRS 2018), Kuala Lumpur, Malaysia, 15–19 October 2018.
59. Dahy, B.; Issa, S.; Ksiksi, T.; Saleous, N. Non-Conventional Methods as a New Alternative for the Estimation of Terrestrial Biomass and Carbon Sequestered: Mini Review. *World J. Agric. Soil Sci.* **2019**. [[CrossRef](#)]
60. Jucker, T.; Caspersen, J.; Chave, J.; Antin, C.; Barbier, N.; Bongers, F.; Dalponte, M.; van Ewijk, K.Y.; Forrester, D.I.; Haeni, M. Allometric equations for integrating remote sensing imagery into forest monitoring programmes. *Glob. Chang. Biol.* **2017**, *23*, 177–190. [[CrossRef](#)] [[PubMed](#)]

61. Saldarriaga, J.G.; West, D.C.; Tharp, M.L.; Uhl, C. Long-term chronosequence of forest succession in the upper Rio Negro of Colombia and Venezuela. *J. Ecol.* **1988**, *938*–958. [[CrossRef](#)]
62. Hughes, R.F.; Kauffman, J.B.; Jaramillo, V.J. Biomass, carbon, and nutrient dynamics of secondary forests in a humid tropical region of Mexico. *Ecology* **1999**, *80*, 1892–1907.
63. Thenkabail, P.S.; Stucky, N.; Griscom, B.W.; Ashton, M.S.; Diels, J.; van der Meer, B.; Enclona, E. Biomass estimations and carbon stock calculations in the oil palm plantations of African derived savannas using IKONOS data. *Int. J. Remote Sens.* **2004**, *25*, 5447–5472. [[CrossRef](#)]
64. Corley, R.H.V.; Tinker, P.B.H. *The Oil Palm*; John Wiley & Sons: Hoboken, NJ, USA, 2008.
65. Dewi, S.; Khasanah, N.; Rahayu, S.; Ekadinata, A.; Van Noordwijk, M. *Carbon Footprint of Indonesian Palm Oil Production: A Pilot Study*; World Agroforestry Centre-ICRAF, SEA Regional Office: Bogor, Indonesia, 2009; Volume 8.
66. Goodman, R.C.; Phillips, O.L.; del Castillo Torres, D.; Freitas, L.; Cortese, S.T.; Monteagudo, A.; Baker, T.R. Amazon palm biomass and allometry. *For. Ecol. Manag.* **2013**, *310*, 994–1004. [[CrossRef](#)]
67. Da Silva, F.; Suwa, R.; Kajimoto, T.; Ishizuka, M.; Higuchi, N.; Kunert, N. Allometric equations for estimating biomass of *Euterpe precatoria*, the most abundant palm species in the Amazon. *Forests* **2015**, *6*, 450–463. [[CrossRef](#)]
68. Zahabu, E.; Mugasha, W.A.; Malimbwi, R.E.; Katani, J.Z. *Allometric Biomass and Volume Models for Coconut Trees*; E&D Vision Publishing Ltd.: Dares Salaam, Tanzania, 2018.
69. Hickey, S.M.; Callow, N.J.; Phinn, S.; Lovelock, C.E.; Duarte, C.M. Spatial complexities in aboveground carbon stocks of a semi-arid mangrove community: A remote sensing height-biomass-carbon approach. *Estuar. Coast. Shelf Sci.* **2018**, *200*, 194–201. [[CrossRef](#)]
70. Deng, S.; Shi, Y.; Jin, Y.; Wang, L. A GIS-based approach for quantifying and mapping carbon sink and stock values of forest ecosystem: A case study. *Energy Procedia* **2011**, *5*, 1535–1545. [[CrossRef](#)]
71. Kamusoko, C.; Aniya, M. Hybrid classification of Landsat data and GIS for land use/cover change analysis of the Bindura district, Zimbabwe. *Int. J. Remote Sens.* **2009**, *30*, 97–115. [[CrossRef](#)]
72. Ardö, J.; Olsson, L. Assessment of soil organic carbon in semi-arid Sudan using GIS and the CENTURY model. *J. Arid Environ.* **2003**, *54*, 633–651. [[CrossRef](#)]
73. Iizuka, K.; Tateishi, R. Estimation of CO₂ sequestration by the forests in Japan by discriminating precise tree age category using remote sensing techniques. *Remote Sens.* **2015**, *7*, 15082–15113. [[CrossRef](#)]
74. Main-Knorn, M.; Moisen, G.G.; Healey, S.P.; Keeton, W.S.; Freeman, E.A.; Hostert, P. Evaluating the remote sensing and inventory-based estimation of biomass in the western Carpathians. *Remote Sens.* **2011**, *3*, 1427–1446. [[CrossRef](#)]
75. Makinde, E.O.; Womiloju, A.A.; Ogundeko, M.O. The geospatial modelling of carbon sequestration in Oluwa Forest, Ondo State, Nigeria. *Eur. J. Remote Sens.* **2017**, *50*, 397–413. [[CrossRef](#)]
76. Pflugmacher, D. *Remote Sensing of Forest Biomass Dynamics Using Landsat-Derived Disturbance and Recovery History and Lidar Data*; Oregon State University: Corvallis, OR, USA, 2011.
77. Hebbar, R.; Ravishankar, H.M.; Subramoniam, S.R.; Uday, R.; Dadhwal, V.K. Object oriented classification of high resolution data for inventory of horticultural crops. *Int. Arch. Photogramm. Remote Sens. Spat. Inf. Sci.* **2014**, *40*, 745. [[CrossRef](#)]
78. Xie, Y.; Sha, Z.; Yu, M. Remote sensing imagery in vegetation mapping: A review. *J. Plant Ecol.* **2008**, *1*, 9–23. [[CrossRef](#)]
79. Bryceson, K.P. Likely locust infestation areas in western New South Wales, Australia, located by satellite. *Geocarto Int.* **1991**, *6*, 21–37. [[CrossRef](#)]
80. Anderson, G.L.; Everitt, J.H.; Richardson, A.J.; Escobar, D.E. Using satellite data to map false broomweed (*Ericameria austrotexana*) infestations on south Texas rangelands. *Weed Technol.* **1993**, *7*, 865–871. [[CrossRef](#)]
81. Clark, M.L.; Roberts, D.A.; Clark, D.B. Hyperspectral discrimination of tropical rain forest tree species at leaf to crown scales. *Remote Sens. Environ.* **2005**, *96*, 375–398. [[CrossRef](#)]
82. Ozdemir, I. Estimating stem volume by tree crown area and tree shadow area extracted from pan-sharpened Quickbird imagery in open Crimean juniper forests. *Int. J. Remote Sens.* **2008**, *29*, 5643–5655. [[CrossRef](#)]
83. Næasset, E.; Økland, T. Estimating tree height and tree crown properties using airborne scanning laser in a boreal nature reserve. *Remote Sens. Environ.* **2002**, *79*, 105–115. [[CrossRef](#)]

84. Popescu, S.C.; Wynne, R.H.; Nelson, R.F. Measuring individual tree crown diameter with lidar and assessing its influence on estimating forest volume and biomass. *Can. J. Remote Sens.* **2003**, *29*, 564–577. [[CrossRef](#)]
85. Song, C.; Dickinson, M.B.; Su, L.; Zhang, S.; Yaussey, D. Estimating average tree crown size using spatial information from Ikonos and QuickBird images: Across-sensor and across-site comparisons. *Remote Sens. Environ.* **2010**, *114*, 1099–1107. [[CrossRef](#)]
86. Shafri, H.Z.; Anuar, M.I.; Seman, I.A.; Noor, N.M. Spectral discrimination of healthy and Ganoderma-infected oil palms from hyperspectral data. *Int. J. Remote Sens.* **2011**, *32*, 7111–7129. [[CrossRef](#)]
87. Henry, M.; Picard, N.; Trotta, C.; Manlay, R.; Valentini, R.; Bernoux, M.; Saint André, L. Estimating tree biomass of sub-Saharan African forests: A review of available allometric equations. *Silva Fenn.* **2011**, *45*, 477–569. [[CrossRef](#)]
88. TSITSI, B. Remote sensing of aboveground forest biomass: A review. *Trop. Ecol.* **2016**, *57*, 125–132.
89. Phiri, D.; Morgenroth, J. Developments in Landsat land cover classification methods: A review. *Remote Sens.* **2017**, *9*, 967. [[CrossRef](#)]
90. Shaharum, N.S.N.; Shafri, H.Z.M.; Gambo, J.; Abidin, F.A.Z. Mapping of Krau Wildlife Reserve (KWR) protected area using Landsat 8 and supervised classification algorithms. *Remote Sens. Appl. Soc. Environ.* **2018**, *10*, 24–35. [[CrossRef](#)]
91. Gilbertson, J.K.; Kemp, J.; Van Niekerk, A. Effect of pan-sharpening multi-temporal Landsat 8 imagery for crop type differentiation using different classification techniques. *Comput. Electron. Agric.* **2017**, *134*, 151–159. [[CrossRef](#)]
92. Jawak, S.D.; Devliyali, P.; Luis, A.J. A comprehensive review on pixel oriented and object oriented methods for information extraction from remotely sensed satellite images with a special emphasis on cryospheric applications. *Adv. Remote Sens.* **2015**, *4*, 177. [[CrossRef](#)]
93. Myint, S.W.; Gober, P.; Brazel, A.; Grossman-Clarke, S.; Weng, Q. Per-pixel vs. object-based classification of urban land cover extraction using high spatial resolution imagery. *Remote Sens. Environ.* **2011**, *115*, 1145–1161. [[CrossRef](#)]
94. Blaschke, T. Object based image analysis for remote sensing. *ISPRS J. Photogramm. Remote Sens.* **2010**, *65*, 2–16. [[CrossRef](#)]
95. Pandit, S.; Tsuyuki, S.; Dube, T. Estimating above-ground biomass in sub-tropical buffer zone community Forests, Nepal, using Sentinel 2 data. *Remote Sens.* **2018**, *10*, 601. [[CrossRef](#)]
96. Wani, A.A.; Joshi, P.K.; Singh, O. Estimating biomass and carbon mitigation of temperate coniferous forests using spectral modeling and field inventory data. *Ecol. Inform.* **2015**, *25*, 63–70. [[CrossRef](#)]
97. Clewley, D.; Lucas, R.; Accad, A.; Armston, J.; Bowen, M.; Dwyer, J.; Pollock, S.; Bunting, P.; McAlpine, C.; Eyre, T. An approach to mapping forest growth stages in Queensland, Australia through integration of ALOS PALSAR and Landsat sensor data. *Remote Sens.* **2012**, *4*, 2236–2255. [[CrossRef](#)]
98. Robinson, C.; Saatchi, S.; Neumann, M.; Gillespie, T. Impacts of spatial variability on aboveground biomass estimation from L-band radar in a temperate forest. *Remote Sens.* **2013**, *5*, 1001–1023. [[CrossRef](#)]
99. Castel, T.; Guerra, F.; Ruiz, A.; Albarran, V.; Caraglio, Y.; Houllier, F. Retrieval biomass of a large Venezuelan pine plantation using JERS-1 SAR data. In Proceedings of the Geoscience and Remote Sensing Symposium, 2000 (IGARSS 2000), Honolulu, HI, USA, 24–28 July 2000; Volume 1, pp. 396–398.
100. Wijaya, A.; Gloaguen, R. Fusion of ALOS Palsar and Landsat ETM data for land cover classification and biomass modeling using non-linear methods. In Proceedings of the Geoscience and Remote Sensing Symposium, 2009 IEEE International (IGARSS 2009), Cape Town, South Africa, 12–17 July 2009; Volume 1, p. III-581.
101. Eisfelder, C.; Kuenzer, C.; Dech, S. Derivation of biomass information for semi-arid areas using remote-sensing data. *Int. J. Remote Sens.* **2012**, *33*, 2937–2984. [[CrossRef](#)]
102. Monteith, J.L. Solar radiation and productivity in tropical ecosystems. *J. Appl. Ecol.* **1972**, *9*, 747–766. [[CrossRef](#)]
103. Rosema, A. Using METEOSAT for operational evapotranspiration and biomass monitoring in the Sahel region. *Remote Sens. Environ.* **1993**, *46*, 27–44. [[CrossRef](#)]
104. Williams, C.A. Integration of remote sensing and modeling to understand carbon fluxes and climate interactions in Africa. In *Ecosystem Function in Savannas: Measurement and Modeling at Landscape to Global Scales*; Hill, M.J., Hanan, N., Eds.; CRC Press: Boca Raton, FL, USA, 2010; pp. 327–346.

105. Morel, A.C.; Fisher, J.B.; Malhi, Y. Evaluating the potential to monitor aboveground biomass in forest and oil palm in Sabah, Malaysia, for 2000–2008 with Landsat ETM+ and ALOS-PALSAR. *Int. J. Remote Sens.* **2012**, *33*, 3614–3639. [[CrossRef](#)]
106. Mutanga, O.; Rugege, D. Integrating remote sensing and spatial statistics to model herbaceous biomass distribution in a tropical savanna. *Int. J. Remote Sens.* **2006**, *27*, 3499–3514. [[CrossRef](#)]
107. Wu, C.; Shen, H.; Wang, K.; Shen, A.; Deng, J.; Gan, M. Landsat imagery-based above ground biomass estimation and change investigation related to human activities. *Sustainability* **2016**, *8*, 159. [[CrossRef](#)]
108. Kelsey, K.C.; Neff, J.C. Estimates of aboveground biomass from texture analysis of Landsat imagery. *Remote Sens.* **2014**, *6*, 6407–6422. [[CrossRef](#)]
109. Chong, K.L.; Kanniah, K.D.; Pohl, C.; Tan, K.P. A review of remote sensing applications for oil palm studies. *Geo-Spat. Inf. Sci.* **2017**, *20*, 184–200. [[CrossRef](#)]
110. McMorrow, J. Linear regression modelling for the estimation of oil palm age from Landsat TM. *Int. J. Remote Sens.* **2001**, *22*, 2243–2264. [[CrossRef](#)]
111. Xiaoming, F.; Yingshi, Z.; Yan, L. Remote sensing linked modeling of the aboveground biomass of semiarid grassland in Inner Mongolia. In Proceedings of the Geoscience and Remote Sensing Symposium, 2005 (IGARSS 2005), Seoul, Korea, 25–29 July 2005; Volume 5, pp. 3047–3050.
112. Tan, K.P.; Kanniah, K.D.; Cracknell, A.P. Use of UK-DMC 2 and ALOS PALSAR for studying the age of oil palm trees in southern peninsular Malaysia. *Int. J. Remote Sens.* **2013**, *34*, 7424–7446. [[CrossRef](#)]
113. Im, J.; Jensen, J.R. Hyperspectral remote sensing of vegetation. *Geogr. Compass* **2008**, *2*, 1943–1961. [[CrossRef](#)]
114. Saganuma, H.; Abe, Y.; Taniguchi, M.; Tanouchi, H.; Utsugi, H.; Kojima, T.; Yamada, K. Stand biomass estimation method by canopy coverage for application to remote sensing in an arid area of Western Australia. *For. Ecol. Manag.* **2006**, *222*, 75–87. [[CrossRef](#)]
115. Greenberg, J.A.; Dobrowski, S.Z.; Ustin, S.L. Shadow allometry: Estimating tree structural parameters using hyperspatial image analysis. *Remote Sens. Environ.* **2005**, *97*, 15–25. [[CrossRef](#)]
116. St-Onge, B.; Hu, Y.; Vega, C. Mapping the height and above-ground biomass of a mixed forest using lidar and stereo Ikonos images. *Int. J. Remote Sens.* **2008**, *29*, 1277–1294. [[CrossRef](#)]
117. Reinartz, P.; Müller, R.; Hoja, D.; Lehner, M.; Schroeder, M. Comparison and fusion of DEM derived from SPOT-5 HRS and SRTM data and estimation of forest heights. In Proceedings of the EARSel Workshop on 3D-Remote Sensing, Porto, Portugal, 10–11 June 2005; Volume 1.
118. Wallerman, J.; Fransson, J.E.; Bohlin, J.; Reese, H.; Olsson, H. Forest mapping using 3D data from SPOT-5 HRS and Z/I DMC. In Proceedings of the 2010 IEEE International Geoscience and Remote Sensing Symposium, Sydney, Australia, 13–16 December 2010; pp. 64–67.
119. Das, S.; Singh, T.P. Correlation analysis between biomass and spectral vegetation indices of forest ecosystem. *Int. J. Eng. Res. Technol.* **2012**, *1*, 1–13.
120. Bannari, A.; Morin, D.; Bonn, F.; Huete, A.R. A review of vegetation indices. *Remote Sens. Rev.* **1995**, *13*, 95–120. [[CrossRef](#)]
121. Patel, N.K.; Saxena, R.K.; Shiwalkar, A. Study of fractional vegetation cover using high spectral resolution data. *J. Indian Soc. Remote Sens.* **2007**, *35*, 73–79. [[CrossRef](#)]
122. Günlü, A.; Ercanli, I.; Başkent, E.Z.; Çakır, G. Estimating aboveground biomass using Landsat TM imagery: A case study of Anatolian Crimean pine forests in Turkey. *Ann. For. Res.* **2014**, *57*, 289–298.
123. Huete, A.R. A soil-adjusted vegetation index (SAVI). *Remote Sens. Environ.* **1988**, *25*, 295–309. [[CrossRef](#)]
124. Baret, F.; Guyot, G.; Major, D.J. TSAVI: A vegetation index which minimizes soil brightness effects on LAI and APAR estimation. In Proceedings of the 12th Canadian Symposium on Remote Sensing Geoscience and Remote Sensing Symposium, Vancouver, BC, Canada, 10–14 July 1989; Volume 3, pp. 1355–1358.
125. Jiang, Z.; Huete, A.R.; Didan, K.; Miura, T. Development of a two-band enhanced vegetation index without a blue band. *Remote Sens. Environ.* **2008**, *112*, 3833–3845. [[CrossRef](#)]
126. Pinty, B.; Verstraete, M.M. GEMI: A non-linear index to monitor global vegetation from satellites. *Vegetatio* **1992**, *101*, 15–20. [[CrossRef](#)]
127. Turner, D.P.; Cohen, W.B.; Kennedy, R.E.; Fassnacht, K.S.; Briggs, J.M. Relationships between leaf area index and Landsat TM spectral vegetation indices across three temperate zone sites. *Remote Sens. Environ.* **1999**, *70*, 52–68. [[CrossRef](#)]

128. Jackson, R.D.; Huete, A.R. Interpreting vegetation indices. *Prev. Vet. Med.* **1991**, *11*, 185–200. [[CrossRef](#)]
129. Sonnenschein, R.; Kuemmerle, T.; Udelhoven, T.; Stellmes, M.; Hostert, P. Differences in Landsat-based trend analyses in drylands due to the choice of vegetation estimate. *Remote Sens. Environ.* **2011**, *115*, 1408–1420. [[CrossRef](#)]
130. Aly, A.A.; Al-Omran, A.M.; Sallam, A.S.; Al-Wabel, M.I.; Al-Shayaa, M.S. Vegetation cover change detection and assessment in arid environment using multi-temporal remote sensing images and ecosystem management approach. *Solid Earth* **2016**, *7*, 713–725. [[CrossRef](#)]
131. Srestasathiern, P.; Rakwatin, P. Oil palm tree detection with high resolution multi-spectral satellite imagery. *Remote Sens.* **2014**, *6*, 9749–9774. [[CrossRef](#)]
132. Zhao, P.; Lu, D.; Wang, G.; Wu, C.; Huang, Y.; Yu, S. Examining spectral reflectance saturation in Landsat imagery and corresponding solutions to improve forest aboveground biomass estimation. *Remote Sens.* **2016**, *8*, 469. [[CrossRef](#)]
133. Mutanga, O.; Skidmore, A.K. Narrow band vegetation indices overcome the saturation problem in biomass estimation. *Int. J. Remote Sens.* **2004**, *25*, 3999–4014. [[CrossRef](#)]
134. Singh, M.; Malhi, Y.; Bhagwat, S. Evaluating land use and aboveground biomass dynamics in an oil palm-dominated landscape in Borneo using optical remote sensing. *J. Appl. Remote Sens.* **2014**, *8*, 083695. [[CrossRef](#)]
135. Gizachew, B.; Solberg, S.; Næsset, E.; Gobakken, T.; Bollandsås, O.M.; Breidenbach, J.; Zahabu, E.; Mauya, E.W. Mapping and estimating the total living biomass and carbon in low-biomass woodlands using Landsat 8 CDR data. *Carbon Balance Manag.* **2016**, *11*, 13. [[CrossRef](#)]
136. Lal, R. Soil carbon dynamics in cropland and rangeland. *Environ. Pollut.* **2002**, *116*, 353–362. [[CrossRef](#)]
137. Montagni, A.; Corona, P.; Dalponte, M.; Gianelle, D.; Chirici, G.; Olsson, H. Airborne laser scanning of forest resources: An overview of research in Italy as a commentary case study. *Int. J. Appl. Earth Obs. Geoinf.* **2013**, *23*, 288–300. [[CrossRef](#)]
138. Ramachandran, A.; Jayakumar, S.; Haroon, R.M.; Bhaskaran, A.; Arockiasamy, D.I. Carbon sequestration: Estimation of carbon stock in natural forests using geospatial technology in the Eastern Ghats of Tamil Nadu, India. *Curr. Sci.* **2007**, 323–331.
139. Cho, M.A.; Mathieu, R.; Asner, G.P.; Naidoo, L.; van Aardt, J.; Ramoelo, A.; Debba, P.; Wessels, K.; Main, R.; Smit, I.P. Mapping tree species composition in South African savannas using an integrated airborne spectral and LiDAR system. *Remote Sens. Environ.* **2012**, *125*, 214–226. [[CrossRef](#)]
140. Holm, A.M.; Cridland, S.W.; Roderick, M.L. The use of time-integrated NOAA NDVI data and rainfall to assess landscape degradation in the arid shrubland of Western Australia. *Remote Sens. Environ.* **2003**, *85*, 145–158. [[CrossRef](#)]
141. Thakur, T.; Swamy, S.L. Analysis of land use, diversity, biomass, C and nutrient storage of a dry tropical forest ecosystem of India using satellite remote sensing and GIS techniques. In Proceedings of the International Forestry and Environment Symposium; University of Sri Jayewardenepura, Nugegoda, Sri Lanka, 26–27 November 2010; Volume 15.
142. Ozdemir, I.; Karnieli, A. Predicting forest structural parameters using the image texture derived from WorldView-2 multispectral imagery in a dryland forest, Israel. *Int. J. Appl. Earth Obs. Geoinf.* **2011**, *13*, 701–710. [[CrossRef](#)]
143. Wang, J.; Chen, J.; Ju, W.; Li, M. IA-SDSS: A GIS-based land use decision support system with consideration of carbon sequestration. *Environ. Model. Softw.* **2010**, *25*, 539–553. [[CrossRef](#)]
144. Gernhardt, S.; Adam, N.; Eineder, M.; Bamler, R. Potential of very high resolution SAR for persistent scatterer interferometry in urban areas. *Ann. GIS* **2010**, *16*, 103–111. [[CrossRef](#)]
145. Li, M.; Tan, Y.; Pan, J.; Peng, S. Modeling forest aboveground biomass by combining spectrum, textures and topographic features. *Front. For. China* **2008**, *3*, 10–15. [[CrossRef](#)]
146. Baumann, G. How to assess rangeland condition in semiarid ecosystems? In *The Indicative Value of Vegetation in the High Atlas Mountains, Morocco*; Universität zu Köln: Cologne, Germany, 2009.
147. Aranha, J.T.; Viana, H.F.; Rodrigues, R. Vegetation classification and quantification by satellite image processing. A case study in North Portugal. In Proceedings of the International Conference and Exhibition on Bioenergy; Universidade do Minho, Guimarães, Portugal, 6–9 April 2008; p. 7.

148. Le Maire, G.; François, C.; Soudani, K.; Berveiller, D.; Pontailier, J.-Y.; Bréda, N.; Genet, H.; Davi, H.; Dufrêne, E. Calibration and validation of hyperspectral indices for the estimation of broadleaved forest leaf chlorophyll content, leaf mass per area, leaf area index and leaf canopy biomass. *Remote Sens. Environ.* **2008**, *112*, 3846–3864. [[CrossRef](#)]
149. Maynard, C.L.; Lawrence, R.L.; Nielsen, G.A.; Decker, G. Modeling vegetation amount using bandwise regression and ecological site descriptions as an alternative to vegetation indices. *GIScience Remote Sens.* **2007**, *44*, 68–81. [[CrossRef](#)]
150. Labrecque, S.; Fournier, R.A.; Luther, J.E.; Piercey, D. A comparison of four methods to map biomass from Landsat-TM and inventory data in western Newfoundland. *For. Ecol. Manag.* **2006**, *226*, 129–144. [[CrossRef](#)]
151. Smith, W.K.; Dannenberg, M.P.; Yan, D.; Herrmann, S.; Barnes, M.L.; Barron-Gafford, G.A.; Biederman, J.A.; Ferrenberg, S.; Fox, A.M.; Hudson, A.; et al. Remote sensing of dryland ecosystem structure and function: Progress, challenges, and opportunities. *Remote Sens. Environ.* **2019**, *233*, 111401. [[CrossRef](#)]
152. Qi, J.; Huete, A.R.; Cabot, F.; Chehbouni, A. Bidirectional properties and utilizations of high-resolution spectra from a semiarid watershed. *Water Resour. Res.* **1994**, *30*, 1271–1279. [[CrossRef](#)]
153. Ritchie, J.C.; Rango, A. Remote sensing applications to hydrology: Introduction. *Hydrol. Sci. J.* **1996**, *41*, 429–431. [[CrossRef](#)]
154. Al-Ahmadi, F.S.; Hames, A.S. Comparison of four classification methods to extract land use and land cover from raw satellite images for some remote arid areas, kingdom of Saudi Arabia. *Earth* **2009**, *20*, 167–190. [[CrossRef](#)]
155. Abburu, S.; Golla, S.B. Satellite image classification methods and techniques: A review. *Int. J. Comput. Appl.* **2015**, *119*. [[CrossRef](#)]
156. Wylie, B.; Denda, I.; Pieper, R.; Harrington, J.; Reed, B.; Southward, G. Satellite-Based Herbaceous Biomass Estimates in the Pastoral Zone of Niger. *J. Range Manag.* **1995**, *48*, 159–164. [[CrossRef](#)]
157. Schucknecht, A.; Meroni, M.; Kayitakire, F.; Rembold, F.; Boureima, A. Biomass estimation to support pasture management in Niger. *Int. Arch. Photogramm. Remote Sens. Spat. Inf. Sci.* **2015**, *40*, 109. [[CrossRef](#)]
158. Tucker, C.J.; Vanpraet, C.L.; Sharman, M.J.; Van Ittersum, G. Satellite remote sensing of total herbaceous biomass production in the Senegalese Sahel: 1980–1984. *Remote Sens. Environ.* **1985**, *17*, 233–249. [[CrossRef](#)]
159. Diouf, A.; Lambin, E.F. Monitoring land-cover changes in semi-arid regions: Remote sensing data and field observations in the Ferlo, Senegal. *J. Arid Environ.* **2001**, *48*, 129–148. [[CrossRef](#)]
160. Olsen, J.L.; Miehe, S.; Ceccato, P.; Fensholt, R. Does EO NDVI seasonal metrics capture variations in species composition and biomass due to grazing in semi-arid grassland savannas? *Biogeosciences* **2015**, *12*, 4407–4419. [[CrossRef](#)]
161. McGwire, K.; Minor, T.; Fenstermaker, L. Hyperspectral mixture modeling for quantifying sparse vegetation cover in arid environments. *Remote Sens. Environ.* **2000**, *72*, 360–374. [[CrossRef](#)]
162. Ren, H.; Zhou, G.; Zhang, X. Estimation of green aboveground biomass of desert steppe in Inner Mongolia based on red-edge reflectance curve area method. *Biosyst. Eng.* **2011**, *109*, 385–395. [[CrossRef](#)]
163. Mangiarotti, S.; Mazzega, P.; Jarlan, L.; Mougou, E.; Baup, F.; Demarty, J. Evolutionary bi-objective optimization of a semi-arid vegetation dynamics model with NDVI and σ_0 satellite data. *Remote Sens. Environ.* **2008**, *112*, 1365–1380. [[CrossRef](#)]
164. Svoray, T.; Shoshany, M. Herbaceous biomass retrieval in habitats of complex composition: A model merging SAR images with unmixed Landsat TM data. *IEEE Trans. Geosci. Remote Sens.* **2003**, *41*, 1592–1601. [[CrossRef](#)]
165. Svoray, T.; Shoshany, M. SAR-based estimation of areal aboveground biomass (AAB) of herbaceous vegetation in the semi-arid zone: A modification of the water-cloud model. *Int. J. Remote Sens.* **2002**, *23*, 4089–4100. [[CrossRef](#)]
166. Svoray, T.; Shoshany, M.; Curran, P.J.; Foody, G.M.; Perevolotsky, A. Relationship between green leaf biomass volumetric density and ERS-2 SAR backscatter of four vegetation formations in the semi-arid zone of Israel. *Int. J. Remote Sens.* **2001**, *22*, 1601–1607. [[CrossRef](#)]
167. Zandler, H.; Brenning, A.; Samimi, C. Quantifying dwarf shrub biomass in an arid environment: Comparing empirical methods in a high dimensional setting. *Remote Sens. Environ.* **2015**, *158*, 140–155. [[CrossRef](#)]

168. Lal, R. Potential of desertification control to sequester carbon and mitigate the greenhouse effect. *Clim. Chang.* **2001**, *51*, 35–72. [[CrossRef](#)]
169. Oldeland, J.; Dorigo, W.; Wesuls, D.; Jürgens, N. Mapping bush encroaching species by seasonal differences in hyperspectral imagery. *Remote Sens.* **2010**, *2*, 1416–1438. [[CrossRef](#)]
170. Tian, F.; Brandt, M.; Liu, Y.Y.; Verger, A.; Tagesson, T.; Diouf, A.A.; Rasmussen, K.; Mbow, C.; Wang, Y.; Fensholt, R. Remote sensing of vegetation dynamics in drylands: Evaluating vegetation optical depth (VOD) using AVHRR NDVI and in situ green biomass data over West African Sahel. *Remote Sens. Environ.* **2016**, *177*, 265–276. [[CrossRef](#)]
171. Bradley, A.V.; Haughan, A.E.; Al-Dughairi, A.; McLaren, S.J. Spatial variability in shrub vegetation across dune forms in central Saudi Arabia. *J. Arid Environ.* **2019**, *161*, 72–84. [[CrossRef](#)]
172. Drake, J.B.; Knox, R.G.; Dubayah, R.O.; Clark, D.B.; Condit, R.; Blair, J.B.; Hofton, M. Above-ground biomass estimation in closed canopy neotropical forests using lidar remote sensing: Factors affecting the generality of relationships. *Glob. Ecol. Biogeogr.* **2003**, *12*, 147–159. [[CrossRef](#)]
173. Carson, H.W.; Lass, L.W.; Callihan, R.H. Detection of yellow hawkweed (*Hieracium pratense*) with high resolution multispectral digital imagery. *Weed Technol.* **1995**, *9*, 477–483. [[CrossRef](#)]
174. Franklin, J.F.; Spies, T.A.; Van Pelt, R.; Carey, A.B.; Thornburgh, D.A.; Berg, D.R.; Lindenmayer, D.B.; Harmon, M.E.; Keeton, W.S.; Shaw, D.C. Disturbances and structural development of natural forest ecosystems with silvicultural implications, using Douglas-fir forests as an example. *For. Ecol. Manag.* **2002**, *155*, 399–423. [[CrossRef](#)]
175. Lunetta, R.S.; Johnson, D.M.; Lyon, J.G.; Crotwell, J. Impacts of imagery temporal frequency on land-cover change detection monitoring. *Remote Sens. Environ.* **2004**, *89*, 444–454. [[CrossRef](#)]
176. Kennedy, R.E.; Ohmann, J.; Gregory, M.; Roberts, H.; Yang, Z.; Bell, D.M.; Kane, V.; Hughes, M.J.; Cohen, W.B.; Powell, S. An empirical, integrated forest biomass monitoring system. *Environ. Res. Lett.* **2018**, *13*, 025004. [[CrossRef](#)]
177. Timothy, D.; Onesimo, M.; Riyad, I. Quantifying aboveground biomass in African environments: A review of the trade-offs between sensor estimation accuracy and costs. *Trop. Ecol.* **2016**, *57*, 393–405.
178. Basuki, T.M.; Van Laake, P.E.; Skidmore, A.K.; Hussin, Y.A. Allometric equations for estimating the above-ground biomass in tropical lowland Dipterocarp forests. *For. Ecol. Manag.* **2009**, *257*, 1684–1694. [[CrossRef](#)]
179. Kajisa, T.; Murakami, T.; Mizoue, N.; Top, N.; Yoshida, S. Object-based forest biomass estimation using Landsat ETM+ in Kampong Thom Province, Cambodia. *J. For. Res.* **2009**, *14*, 203–211. [[CrossRef](#)]
180. Hame, T.; Salli, A.; Andersson, K.; Lohi, A. A new methodology for the estimation of biomass of conifer-dominated boreal forest using NOAA AVHRR data. *Int. J. Remote Sens.* **1997**, *18*, 3211–3243. [[CrossRef](#)]
181. He, Q. Estimation of coniferous forest above-ground biomass using LiDAR and SPOT-5 data. In Proceedings of the 2012 2nd Remote Sensing, Environment and Transportation Engineering (RSETE), Nanjing, China, 1–3 June 2012; pp. 1–4.
182. Basuki, T.M.; Skidmore, A.K.; Hussin, Y.A.; Van Duren, I. Estimating tropical forest biomass more accurately by integrating ALOS PALSAR and Landsat-7 ETM+ data. *Int. J. Remote Sens.* **2013**, *34*, 4871–4888. [[CrossRef](#)]
183. Jones, M.O.; Jones, L.A.; Kimball, J.S.; McDonald, K.C. Satellite passive microwave remote sensing for monitoring global land surface phenology. *Remote Sens. Environ.* **2011**, *115*, 1102–1114. [[CrossRef](#)]
184. Brandt, M.; Wigneron, J.-P.; Chave, J.; Tagesson, T.; Penuelas, J.; Ciais, P.; Rasmussen, K.; Tian, F.; Mbow, C.; Al-Yaari, A. Satellite passive microwaves reveal recent climate-induced carbon losses in African drylands. *Nat. Ecol. Evol.* **2018**, *2*, 827–835. [[CrossRef](#)]
185. Baker, N.R. Chlorophyll fluorescence: A probe of photosynthesis in vivo. *Annu. Rev. Plant. Biol.* **2008**, *59*, 89–113. [[CrossRef](#)] [[PubMed](#)]
186. Anderson, M.C.; Allen, R.G.; Morse, A.; Kustas, W.P. Use of Landsat thermal imagery in monitoring evapotranspiration and managing water resources. *Remote Sens. Environ.* **2012**, *122*, 50–65. [[CrossRef](#)]
187. Aubrecht, D.M.; Helliker, B.R.; Goulden, M.L.; Roberts, D.A.; Still, C.J.; Richardson, A.D. Continuous, long-term, high-frequency thermal imaging of vegetation: Uncertainties and recommended best practices. *Agric. For. Meteorol.* **2016**, *228*, 315–326. [[CrossRef](#)]

188. Asner, G.P.; Brodrick, P.G.; Anderson, C.B.; Vaughn, N.; Knapp, D.E.; Martin, R.E. Progressive forest canopy water loss during the 2012–2015 California drought. *Proc. Natl. Acad. Sci. USA* **2016**, *113*, E249–E255. [[CrossRef](#)]
189. Garbulsky, M.F.; Peñuelas, J.; Gamon, J.; Inoue, Y.; Filella, I. The photochemical reflectance index (PRI) and the remote sensing of leaf, canopy and ecosystem radiation use efficiencies: A review and meta-analysis. *Remote Sens. Environ.* **2011**, *115*, 281–297. [[CrossRef](#)]
190. Schneider, F.D.; Morsdorf, F.; Schmid, B.; Petchey, O.L.; Hueni, A.; Schimel, D.S.; Schaepman, M.E. Mapping functional diversity from remotely sensed morphological and physiological forest traits. *Nat. Commun.* **2017**, *8*, 1–12. [[CrossRef](#)]



© 2020 by the authors. Licensee MDPI, Basel, Switzerland. This article is an open access article distributed under the terms and conditions of the Creative Commons Attribution (CC BY) license (<http://creativecommons.org/licenses/by/4.0/>).

© 2020. This work is licensed under <http://creativecommons.org/licenses/by/3.0/> (the “License”). Notwithstanding the ProQuest Terms and Conditions, you may use this content in accordance with the terms of the License.